NASA TECHNICAL MEMORANDUM

NASA TM X-2206

LOW-SUBSONIC AERODYNAMIC CHARACTERISTICS OF A SHUTTLE-ORBITER CONFIGURATION WITH A VARIABLE-DIHEDRAL DELTA WING

by George M. Ware and Bernard Spencer, Jr.

Langley Research Center
Hampton, Va. 23365

1. Report No. NASA TM X-2206	2. Government Accession No.	3. Recipient's Catalog No.
4. Title and Subtitle LOW-SUBSONIC AERODYNAMIC CHARACTERISTICS OF A SHUTTLE-ORBITER CONFIGURATION WITH A VARIABLE-DIHEDRAL DELTA WING		5. Report Date January 1971
		6. Performing Organization Code
7. Author(s) George M. Ware and Bernard Spencer, Jr.		8. Performing Organization Report No. L-7566
9. Performing Organization Name and Address NASA Langley Research Center Hampton, Va. 23365		10. Work Unit No. 124-07-24-05
		11. Contract or Grant No.
12. Sponsoring Agency Name and Address National Aeronautics and Space Administration Washington, D.C. 20546		13. Type of Report and Period Covered Technical Memorandum
		14. Sponsoring Agency Code

15. Supplementary Notes

16. Abstract

An investigation has been conducted in the Langley low-turbulence pressure tunnel to determine the subsonic aerodynamic characteristics of a shuttle-orbiter configuration with a variable-dihedral delta wing. The tests were made at Reynolds numbers, based on body length, of 4.50×10^6 to 26.54×10^6; the angles of attack varied from about -4° to 20° at 0° and 5° of sideslip. The variables investigated included the effects of wing dihedral angle, elevon deflection for pitch and roll control, and vertical-tail size.

17. Key Words (Suggested by Author(s)) Orbiter Variable geometry Aerodynamic data	18. Distribution Statement Unclassified – Unlimited		
19. Security Classif. (of this report) Unclassified	20. Security Classif. (of this page) Unclassified	21. No. of Pages 43	22. Price* $3.00

Page Intentionally Left Blank

LOW-SUBSONIC AERODYNAMIC CHARACTERISTICS OF A

SHUTTLE-ORBITER CONFIGURATION WITH

A VARIABLE-DIHEDRAL DELTA WING

By George M. Ware and Bernard Spencer, Jr.
Langley Research Center

SUMMARY

An investigation has been conducted in the Langley low-turbulence pressure tunnel to determine the subsonic aerodynamic characteristics of a shuttle-orbiter configuration with a variable-dihedral delta wing. For most of the tests, the wings were horizontal, which is the normal position for subsonic cruise. The tests were conducted at Mach numbers less than 0.35 over a range of Reynolds number, based on body length, of 4.50×10^6 to 26.53×10^6. The angle of attack was varied from about -4° to 20° at 0° and 5° of sideslip.

The results of the investigation indicated that increasing the Reynolds number from 4.50×10^6 to 26.53×10^6 had little effect on the lift or stability characteristics of the model but did decrease drag values so that the maximum untrimmed lift-drag ratio increased from 5.6 to 6.1. The model was longitudinally stable about the test center-of-gravity position of 0.70 body length with a static margin of 0.07 body length. By use of the wing-mounted elevons for trim, the model with a static margin of 0.07 body length had a maximum trimmed lift-drag ratio of about 4.0. Deflecting the body base flap -15° in conjunction with the elevons gave a maximum trimmed lift-drag ratio of 4.2. Reducing the static margin to 0.03 body length (i.e., a rearward shift in the assumed center-of-gravity location to 0.74 body length), a value which would more nearly correspond to a vehicle of this type, caused an increase of about 1.0 in the maximum trimmed lift-drag ratio. The fact that the configuration has stable trim characteristics at these center-of-gravity locations is important because in the landing condition, shuttle designs generally have far aft center-of-gravity locations. The model was directionally stable over most of the angle-of-attack range and had large values of effective dihedral. Differential elevon deflection produced constant values of rolling moment with favorable yawing moments over the test range.

INTRODUCTION

The National Aeronautics and Space Administration and the aerospace industry are currently investigating, both experimentally and analytically, configurations suitable for transportation of large payloads to and from near-earth orbit. The basic concept as presently envisioned consists of vertically launched booster and orbiter elements with both stages capable of horizontal landing upon return. The present study presents low-subsonic aerodynamic characteristics of a preliminary design orbiter element which may offer the capability of meeting either the high or low cross-range requirements by use of variable-dihedral wings, since the use of variable-dihedral lifting surfaces has indicated a wide range of trim angles of attack at hypersonic speeds. (See ref. 1.) In addition, partial deployment of these wings contributes significantly to directional stability at hypersonic speeds, the positive increment being a function of toe-in angle as well as dihedral angle.

The present tests were made in the Langley low-turbulence pressure tunnel. Most of the tests were conducted at a Reynolds number, based on body length, of 22.13×10^6 and a Mach number of 0.23 for an angle-of-attack range from about -4° to 20° at 0° and 5° of sideslip. The effects of wing elevon deflection, wing dihedral angle at 0° toe-in, and deflection of the body base flap on the aerodynamic characteristics were investigated.

SYMBOLS

The longitudinal characteristics are presented about the stability axes, and the lateral characteristics are presented about the body axes. All coefficients are normalized with respect to the projected planform area (0.067 m^2), length (57.15 cm), or span (23.88 cm) of the body alone (wings excluded). The moment reference point corresponded to a center-of-gravity location at 0.70 body length.

b   reference span (maximum body span), m

C_D drag coefficient, $\dfrac{\text{Drag}}{qS}$

C_L lift coefficient, $\dfrac{\text{Lift}}{qS}$

C_l rolling-moment coefficient, $\dfrac{\text{Rolling moment}}{qSb}$

$C_{l_\beta} = \dfrac{\Delta C_l}{\Delta \beta}$, per deg

C_m pitching-moment coefficient, $\dfrac{\text{Pitching moment}}{qS\ell}$

$C_{m,o}$ pitching-moment coefficient at zero lift

C_n yawing-moment coefficient, $\dfrac{\text{Yawing moment}}{qSb}$

$C_{n_\beta} = \dfrac{\Delta C_n}{\Delta \beta}$, per deg

C_Y side-force coefficient, $\dfrac{\text{Side force}}{qS}$

$C_{Y_\beta} = \dfrac{\Delta C_Y}{\Delta \beta}$, per deg

L/D lift-drag ratio

ℓ length of body, m

q dynamic pressure, N/m^2

R Reynolds number based on body length

S projected planform of body alone, m^2

α angle of attack, deg

β angle of sideslip, deg

Γ wing dihedral angle (positive with wing tip up), deg

δ_e elevon deflection angle (positive when trailing edge deflected down), deg

δ_f base-flap deflection angle (positive when trailing edge deflected down), deg

Subscripts:

L left

R right

Configuration components:

B   body

W   wing

V   small vertical tail

V_1 large vertical tail

DESCRIPTION OF MODEL

Sketches and photographs of the model used in the investigation are presented in figures 1 and 2, respectively. The model lower body was semicircular at the nose and became a circular arc as the body flared rearward to form a highly swept delta planform. The cross section of the upper body varied from semicircular at the nose to trapezoidal at the rear and did not flare as did the lower body. The juncture of the upper and lower body shapes, therefore, formed triangular horizontal planes aft of about the 0.50 body station, upon which the 58° swept variable-dihedral wings were mounted. In theory, the flared lower body is designed to give the configuration hypersonic trim at high angles of attack (60° to 70°) with the wings at the maximum dihedral angle, to act as a heat shield for the powered hinges of the wings during reentry, and to be used as a storage area for fuel or airbreathing engines. On this model, the wings could be tested at dihedral angles of 0°, 30°, 60°, 90°, and 110° at 0° of toe-in. The model was tested with two sizes of center-mounted vertical tails. For control surfaces, the model had elevons in the wing trailing edge and a base flap in the aft 10 percent of the body.

TESTS AND CORRECTIONS

Tests were made in the Langley low-turbulence pressure tunnel at Reynolds numbers, based on body length, ranging from 4.50×10^6 to 26.53×10^6 at Mach numbers always below 0.35. The angle of attack was varied from about -4° to 20° at 0° and 5° of sideslip.

The model was sting supported, as shown in figure 2(f). The balance and sting were calibrated for the effects of bending in both the longitudinal and lateral planes under combinations of loads. In all cases the drag represents gross drag, in that base drag is included. No wind-tunnel corrections were applied to the data of the present investigation.

4

RESULTS AND DISCUSSION

Because of the preliminary nature of the configuration investigated, no detailed analysis of the results is presented. However, several areas of aerodynamic interest are briefly discussed.

Longitudinal Aerodynamic Characteristics

Effect of Reynolds number.- The effect of increasing Reynolds number on the longitudinal aerodynamic characteristics of the model is presented in figure 3. These data indicate that increasing the Reynolds number caused no change in lift-curve slope or stability level at angles of attack below about 16° and only minor changes in these parameters at higher angles of attack. The drag values, however, decreased with increasing Reynolds number and caused an increase in maximum untrimmed lift-drag ratio from 5.6 at $R = 4.50 \times 10^6$ to 6.1 at $R = 26.53 \times 10^6$. The most significant changes in drag had occurred below $R = 22.13 \times 10^6$, and in order to expedite testing, the rest of the tests were conducted at this value.

Model buildup characteristics.- Data for the complete model, wing-body combination, and body alone are presented in figure 4. The complete model was quite stable longitudinally (static margin of about 0.07 body length) with the center of gravity at 0.70 body length and had a negative pitching moment at zero lift. Addition of a larger vertical tail V_1 produced slightly higher untrimmed lift-drag ratios than the values obtained with the model and the original tail V. This increase in L/D value resulted from the boattailed base of V_1, which caused less drag than the blunt base of V. (See fig. 1.) As would be expected, the model with wings removed had a lower lift-curve slope, maximum lift, and lift-drag ratio, and was longitudinally unstable. It should be noted that no attempt was made to fair the juncture between the body and wings of the model or the wing-body juncture when the wings were removed. As a result, the drag values may be somewhat higher than might be expected for a finalized configuration.

Effect of pitch control deflections.- The effect of elevon deflection, base-flap deflection, and elevon deflection with a base-flap deflection of -15° on the longitudinal characteristics of the model is presented in figures 5, 6, and 7, respectively. Figure 5 shows that the model lift and pitching moment remained relatively linear with elevon deflection and that because of the high level of longitudinal stability and the negative $C_{m,o}$, full negative elevon deflection (-30°) could trim the model to an angle of attack of only about 16°. In an attempt to improve the trim characteristics by increasing the value of $C_{m,o}$, a base flap was added to the model. Deflection of the base flap (fig. 6) was effective in producing positive increments in pitching moment; a deflection of -15° resulted in trim at $C_L = 0$. With a deflection of -15°, however, there was some flow

separation at the flap, as indicated by the large increase in drag and the loss in lift-drag ratio. Flow separation associated with base flaps has been noted in previous investigations. (See ref. 2.) Elevon deflection in conjunction with a base-flap deflection of -15° (fig. 7) allowed trim with $\delta_e = -30^O$ to an angle of attack of about 20°.

Preliminary weight distribution and loading studies of shuttle booster and orbiter elements have indicated that the center of gravity of these vehicles in the return-to-earth configuration will be considerably aft of the 0.60 body station. This aft center-of-gravity position is caused by the heavy rocket engines at the vehicle base and the expenditure of rocket fuel for boost into orbit. As a result, the present configuration was designed for a center-of-gravity position of 0.70 body length. The longitudinal stability data of the preceding figures, however, have shown the stability level to be excessively high. The data of figures 5 and 7 are therefore replotted as figure 8 with the center of gravity moved to 0.74 body length, which should be favorable from the weight distribution standpoint and produce a longitudinal stability value (0.03 body length static margin) which more nearly corresponds to a vehicle of this type.

Trim characteristics.- The control data of figures 5, 7, and 8 are summarized in figure 9 as the variation of trimmed lift-drag values with lift coefficient. Curves are shown for the model, both with and without base-flap deflection. With a value of static margin of 0.07 body length (c.g. at $0.70l$), the model with the small vertical tail V reached a maximum lift-drag value of about 3.9 and a lift coefficient of 0.55. Deflecting the base flap allowed the model to be trimmed to a lift coefficient of about 0.650 and a lift-drag ratio of 4.2. A rearward shift in the center of gravity to $0.74l$ reduced the longitudinal stability and thereby reduced the elevon deflection required for trim. This shift also resulted in an increase of about 1.0 in the maximum trimmed lift-drag ratio. The maximum lift-drag values were, therefore, about 5.0 and 5.1 occurring at a lift coefficient of about 0.53 for the model with base-flap deflection of 0° and -15°, respectively.

Effect of wing dihedral angle.- Although it is envisioned that the variable-dihedral configuration would operate at low subsonic speeds with the wings at a dihedral angle of 0° only, it was of general interest to determine the characteristics of the model over the entire range of wing dihedral angles ($\Gamma = 0^O$ to 110°). These data, presented in figure 10, show that there was a loss in lift, lift-drag ratio, and longitudinal stability as the dihedral angle was increased. With the wings folded to 90°, the model had neutral longitudinal stability with the center of gravity at 0.70 body length and was trimmed between lift coefficients of about 0.15 to 0.47 with lift-drag values from about 2.0 to 2.6. With the wings folded to 110°, the model became longitudinally unstable and had lift characteristics similar to those of the body alone (fig. 4).

6

Lateral Aerodynamic Characteristics

Model buildup characteristics.- The lateral-directional stability characteristics of the model are presented as the variation of the stability derivatives C_{Y_β}, C_{n_β}, and C_{l_β} with angle of attack in figure 11. These data were obtained by taking the difference in lateral coefficients measured at angles of sideslip of 0° and 5° over the test angle-of-attack range and therefore do not account for any nonlinearities which may occur in the intermediate β range.

The model with the original vertical tail V and $\Gamma = 0^O$ had low directional stability over most of the angle-of-attack range, with the stability decreasing to zero at $\alpha = 19^O$. Increasing the tail size (V_1) increased the directional stability of the model over the angle-of-attack range except at angles near 14°, where directional instability occurred. The model, however, regained directional stability at higher angles of attack. Tuft studies, made in an attempt to determine the cause of the reduced stability, indicated that at about $\alpha = 12^O$, a strong vortex was shed from the leading edge of the windward wing at the juncture of the wing and flared body. The resultant flow then swept the body and lower part of the vertical tail, and the negative pressures which were thereby created on the windward side produced the destabilizing effect. No attempt was made to improve the flow, but a smooth fairing of the juncture of the wing and flared body could possibly reduce or eliminate the losses noted in directional stability.

The model with either size vertical tail had high values of the effective dihedral parameter $-C_{l_\beta}$, which together with the relatively low values of C_{n_β} indicate the possibility of low Dutch roll damping characteristics. Longitudinal trim considerations suggest that the center of gravity be moved from 0.70 to 0.74 body length. This movement, however, would result in some loss in directional stability.

Effect of wing dihedral angle.- The effect of wing dihedral angle on the lateral-directional characteristics of the model with the large vertical tail V_1 is presented in figure 12. The characteristics of the model with $\Gamma = 0^O$ (wings horizontal) have been previously discussed. The directional stability of the model generally increased as wing dihedral angle was increased from 0° to 110° over most of the angle-of-attack range. The abrupt increase in directional stability at about $\alpha = 12^O$ for the $\Gamma = 30^O$ wing configuration was evidently the result of a favorable interaction of the vortex of the wing-body juncture with the vertical tail, which was destabilizing when the wings were horizontal. The effects of the vortex disappeared as the wing dihedral angle was increased to 90°. The model had positive effective dihedral characteristics at all of the wing dihedral angles over the angle-of-attack range. Increasing the wing dihedral increased $-C_{l_\beta}$ except for the $\Gamma = 110^O$ configuration, which generally gave values below those for $\Gamma = 0^O$ but appreciably higher than those noted for the body alone (fig. 11).

Lateral control characteristics.- The effect of differential elevon deflection as a roll control is presented in figure 13. These data are for a differential elevon deflection of ±10° from a trim condition with the elevons initially set at -20° for the model with either vertical tail. The data show that differential deflection produced almost constant values of rolling moment over the angle-of-attack range and that the model with the large vertical tail had slightly higher values. Yawing moments were produced in conjunction with the rolling moments. They were, however, in a favorable direction. It may also be noted that the base flap, which was deflected for the tests with the large-vertical-tail model, had little effect on lateral control.

SUMMARY OF RESULTS

Subsonic wind-tunnel tests have been made to determine the static longitudinal and lateral aerodynamic characteristics of a shuttle-orbiter configuration with a variable-dihedral delta wing over angles of attack from about -4° to 20°. For most of the tests, the wings were in the horizontal position. The results of the investigation may be summarized as follows:

1. Increasing Reynolds number from 4.50×10^6 to 26.53×10^6 had little effect on the lift or stability characteristics of the model but did decrease drag values so that there was a resultant increase from 5.6 to 6.1 in maximum untrimmed lift-drag ratio.

2. The model was longitudinally stable about the test center-of-gravity position of 0.70 body length with a static margin of 0.07 body length.

3. By use of the wing-mounted elevons for trim, the model with a static margin of 0.07 body length had a maximum trimmed lift-drag ratio of about 4.0. Deflecting the body base flap -15° in conjunction with the elevons resulted in a maximum trimmed lift-drag ratio of 4.2.

4. Reducing the static margin to 0.03 body length (i.e., a rearward shift of the assumed center-of-gravity location to 0.74 body length), a value which would more nearly correspond to a vehicle of this type, resulted in an increase of about 1.0 in the maximum trimmed lift-drag ratio. The fact that the configuration has stable trim characteristics at these c.g. locations is important because in the landing condition, shuttle designs generally have far aft center-of-gravity locations.

5. The model was directionally stable over most of the angle-of-attack range and had large values of effective dihedral.

6. Differential elevon deflection produced constant values of rolling moment with favorable yawing moments over the test range.

Langley Research Center,
    National Aeronautics and Space Administration,
        Hampton, Va., December 14, 1970.

REFERENCES

1. Spencer, Bernard, Jr.: Hypersonic Aerodynamic Characteristics of a Model of a Low-Fineness-Ratio Variable-Geometry Logistics Spacecraft Concept. NASA TM X-1701, 1968.

2. Spencer, Bernard, Jr.: Low-Speed Longitudinal Aerodynamic Characteristics of a Model of a Blunt-Nose Hypersonic Lifting Spacecraft Having Variable-Sweep Wings. NASA TM X-2102, 1971.
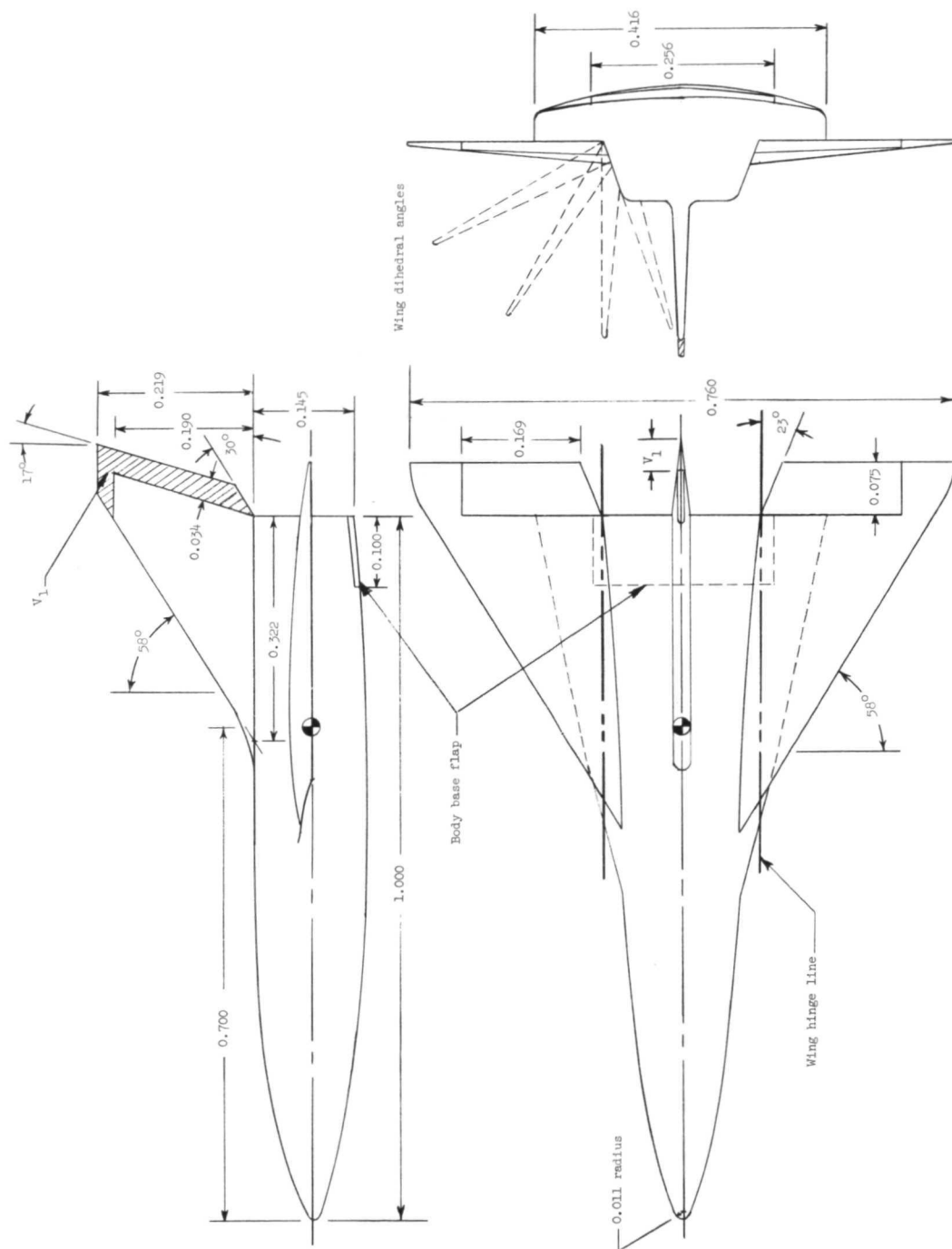
Figure 1.- Sketches of model used in investigation. All dimensions are normalized with respect to body length. Body length = 57.15 cm.

(a) $\Gamma = 0°$.

L-70-4586
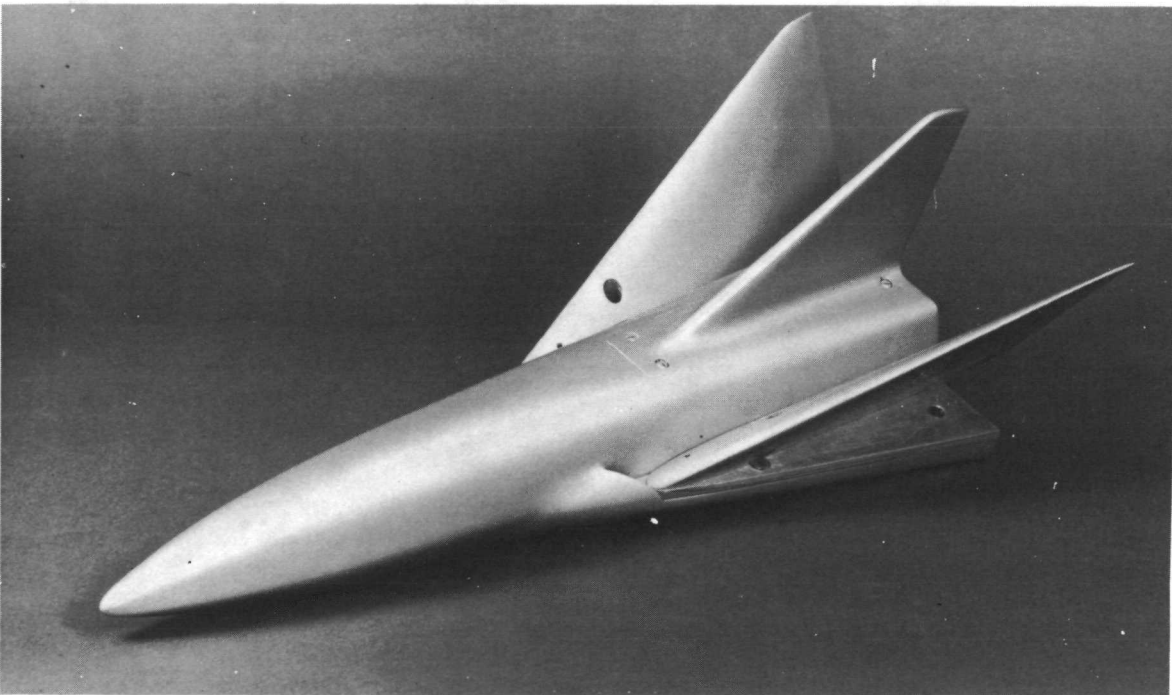
(b) $\Gamma = 60°$.

L-70-4585

Figure 2.- Photographs of model.
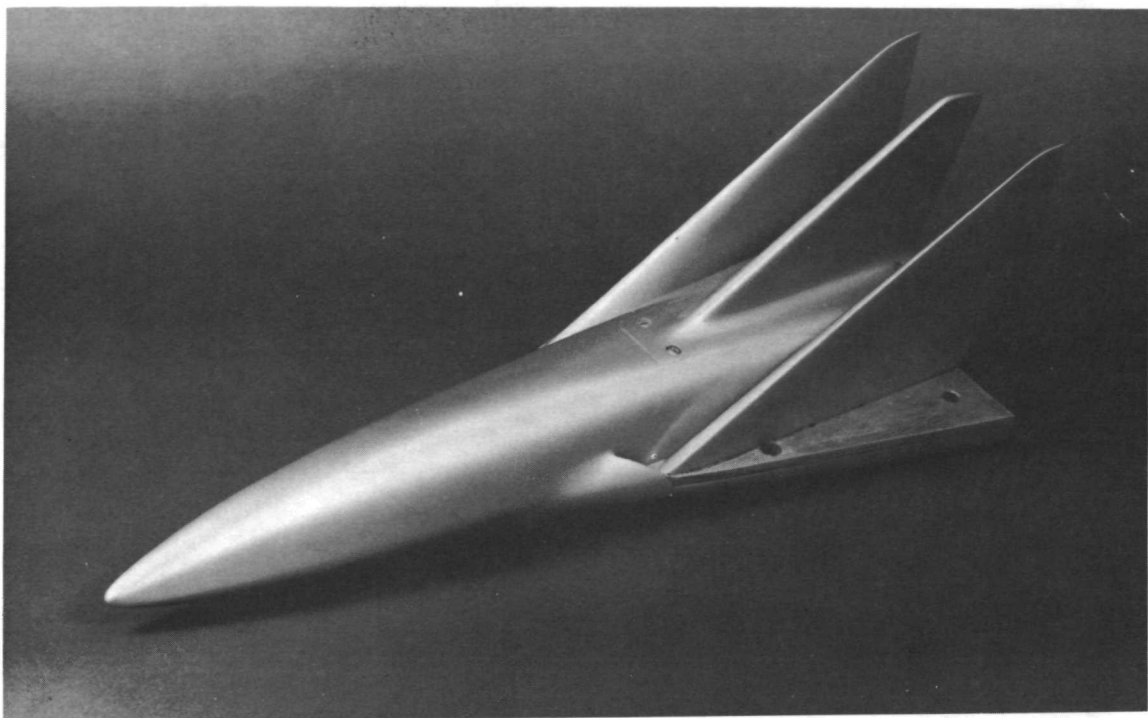
(c) $\Gamma = 90^{\circ}$.

L-70-4582
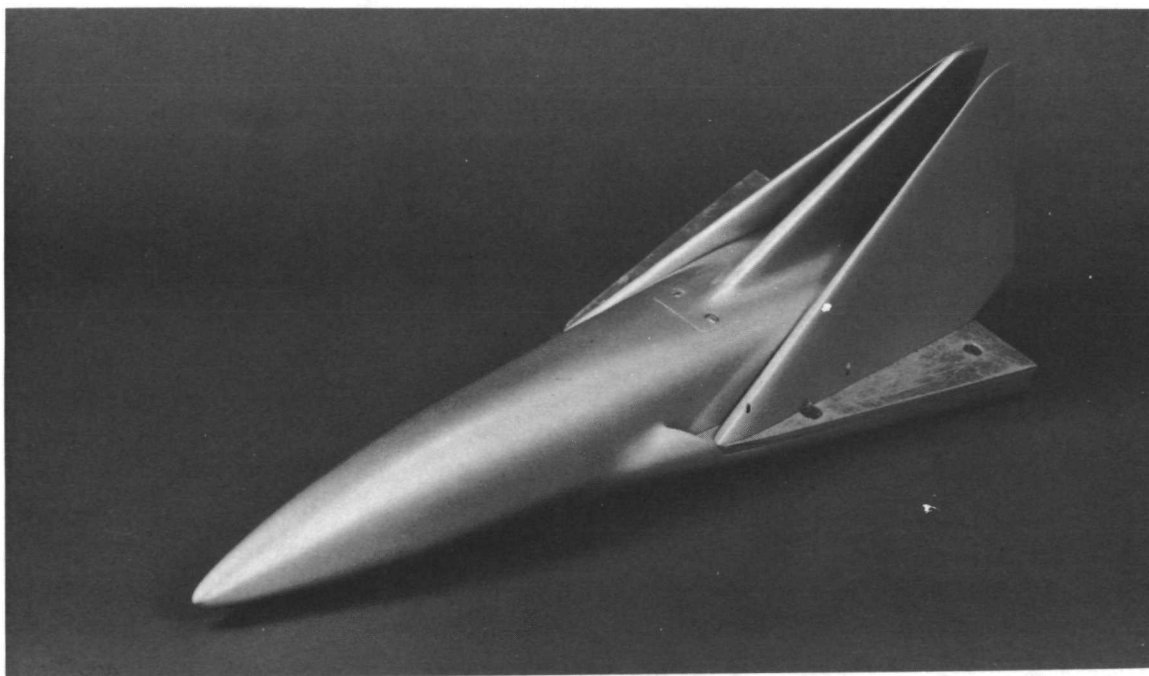
(d) $\Gamma = 110^{\circ}$.

L-70-4583

Figure 2.- Continued.

12
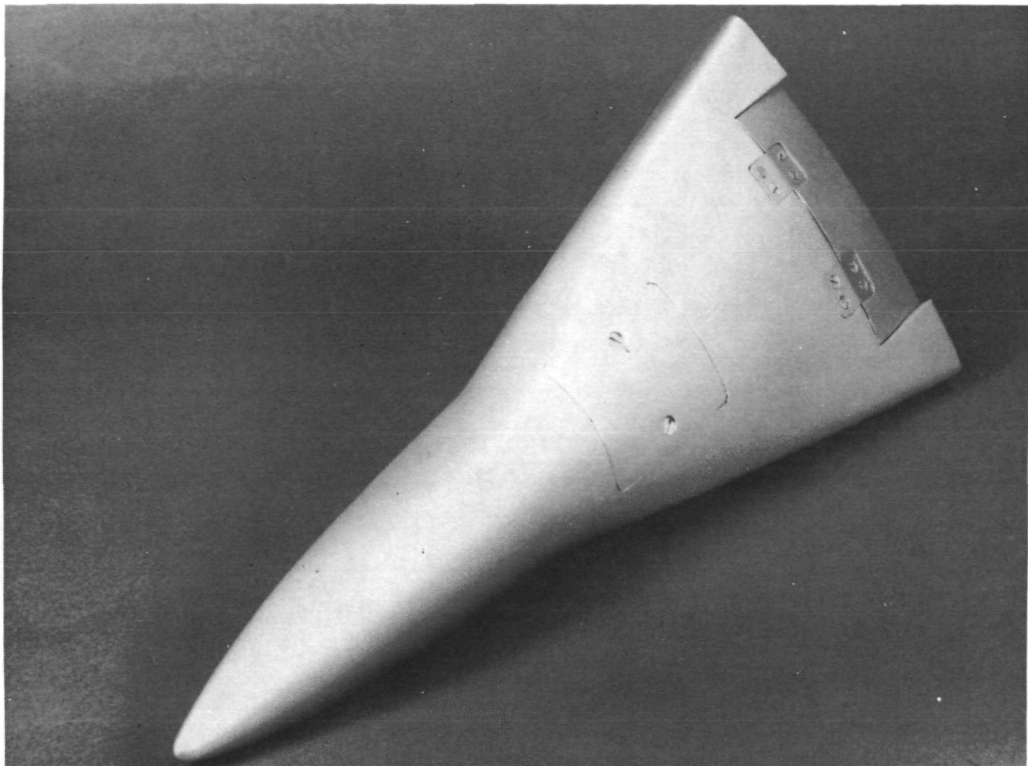
(e) Base flap.

L-70-4584

(f) Model mounted in tunnel.

L-70-4801

Figure 2.- Concluded.

13
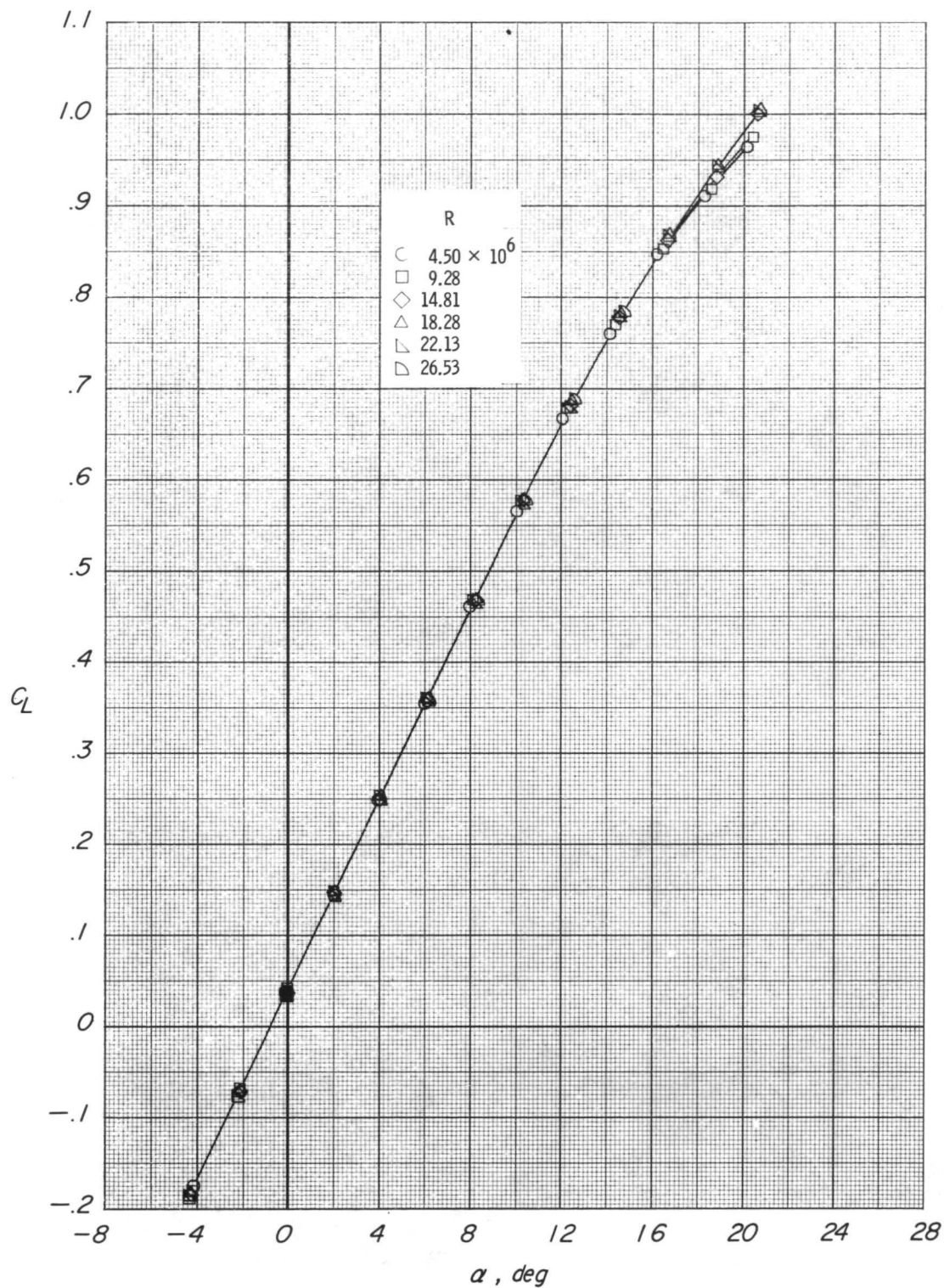
(a) Variation of lift coefficient with angle of attack.

Figure 3.- Effect of increasing Reynolds number on longitudinal aerodynamic characteristics of model. $\Gamma = 0^{\circ}$; $\beta = 0^{\circ}$; $\delta_f = 0^{\circ}$.
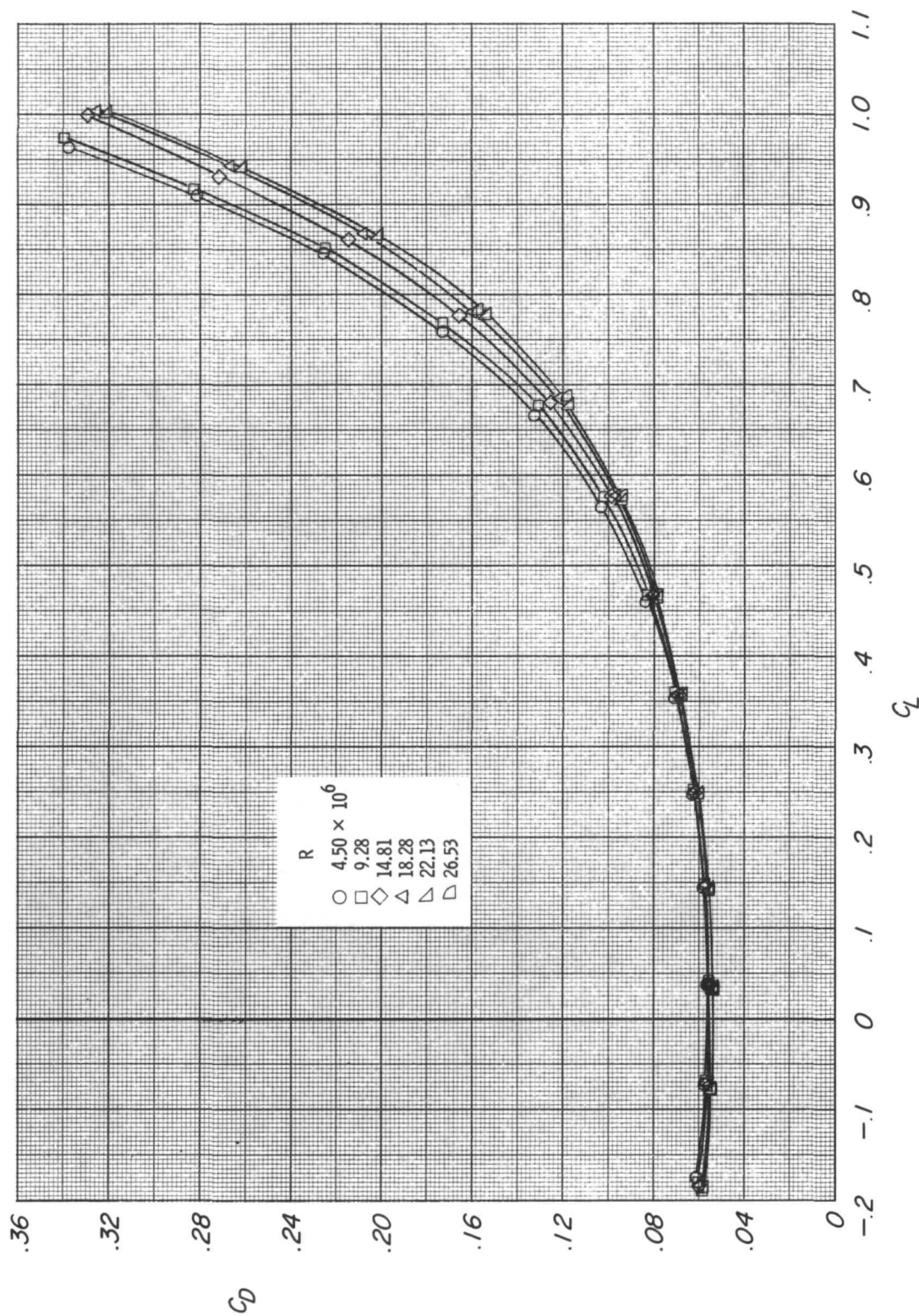
(b) Variation of drag coefficient with lift coefficient.

Figure 3.- Continued.
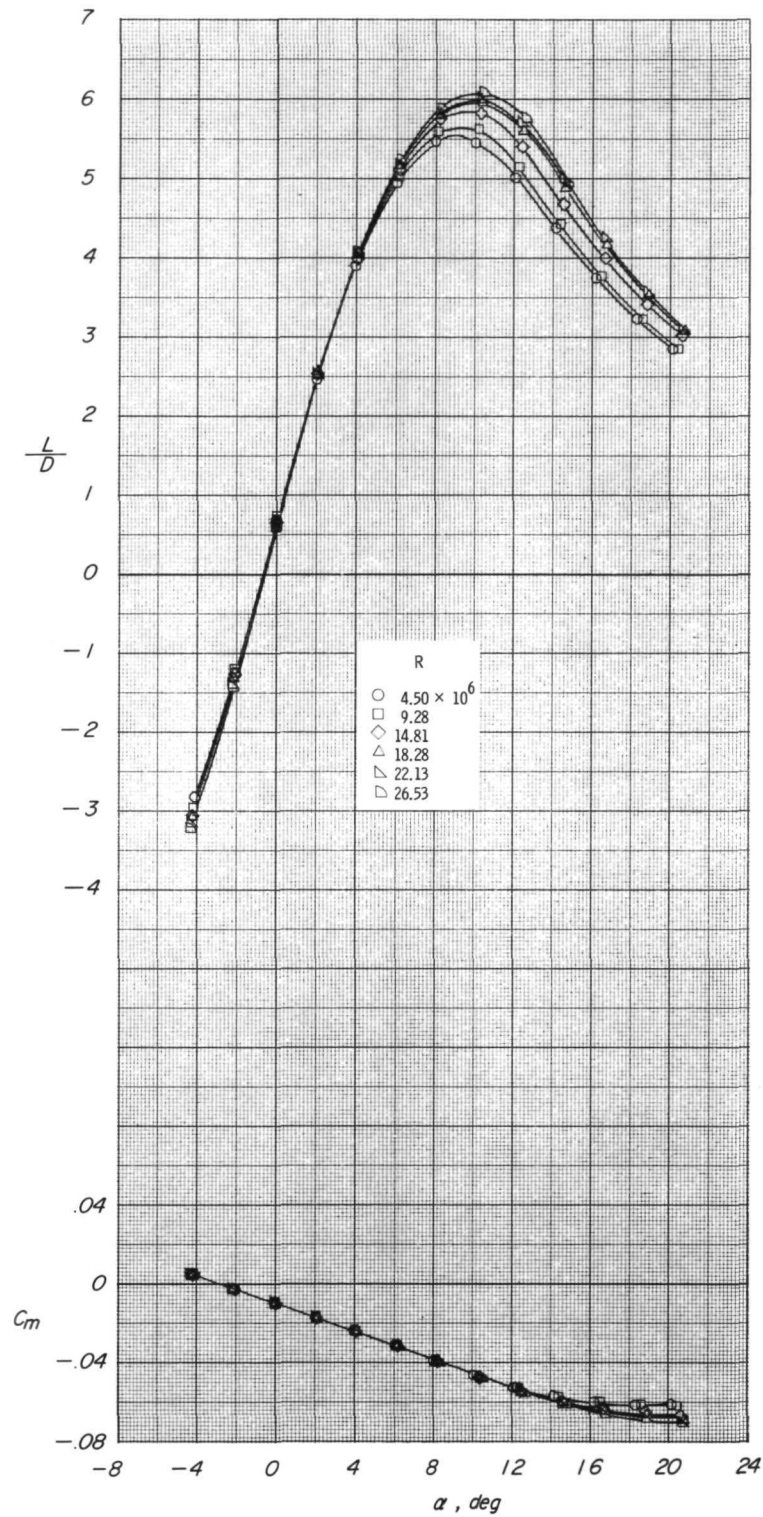
(c) Variation of lift-drag ratio and pitching-moment
coefficient with angle of attack.

Figure 3.- Continued.
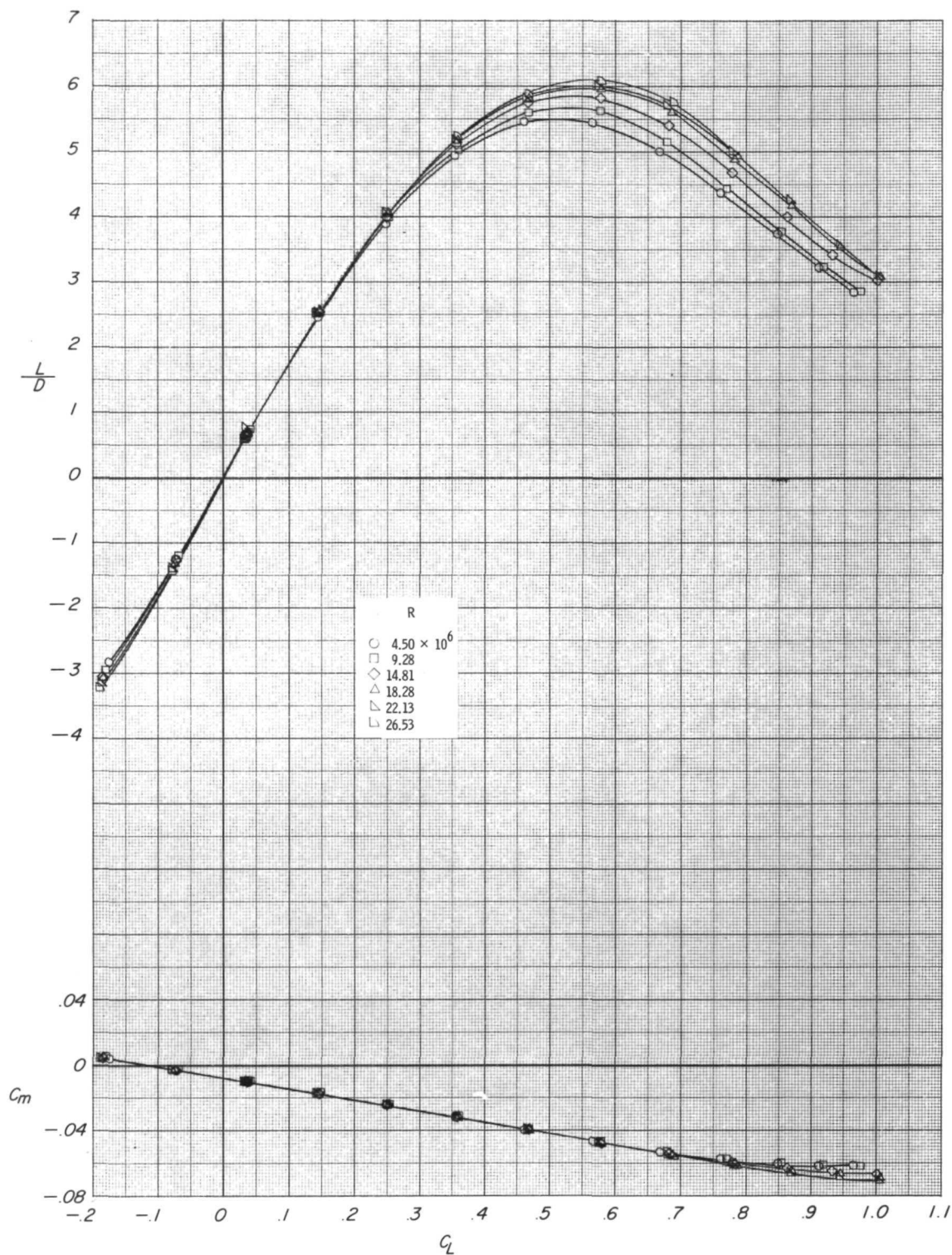
(d) Variation of lift-drag ratio and pitching-moment coefficient with lift coefficient.
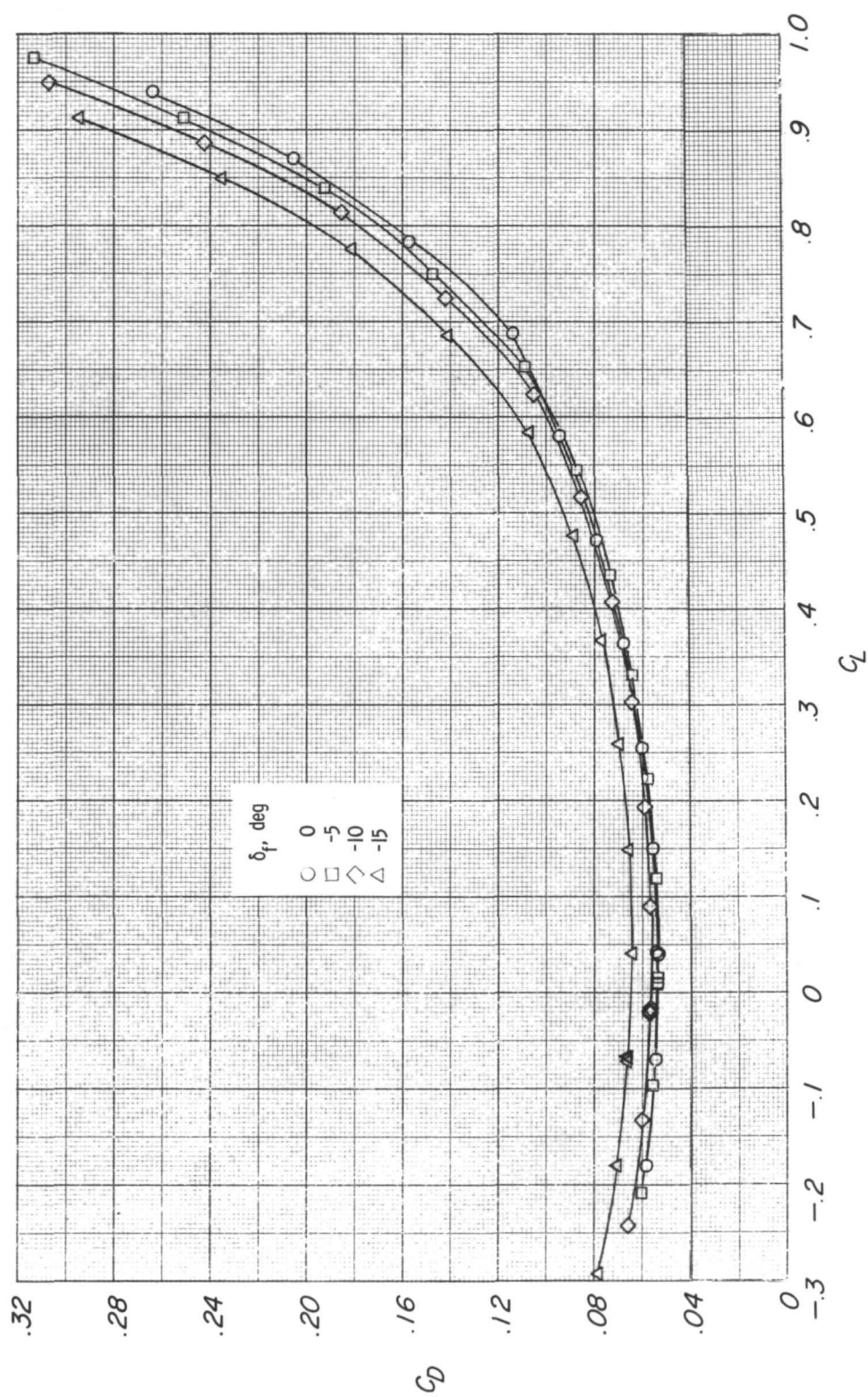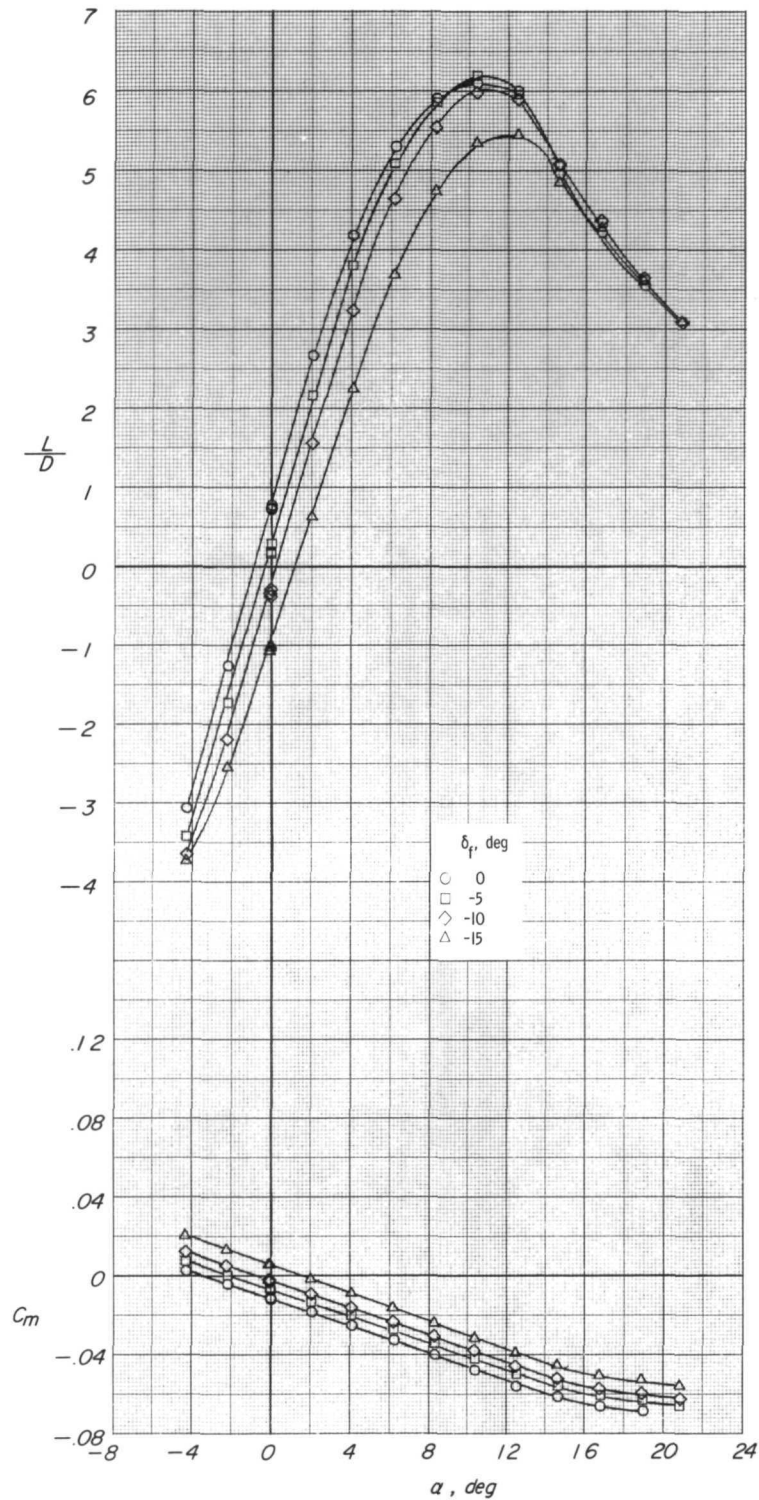
Figure 3.- Concluded.
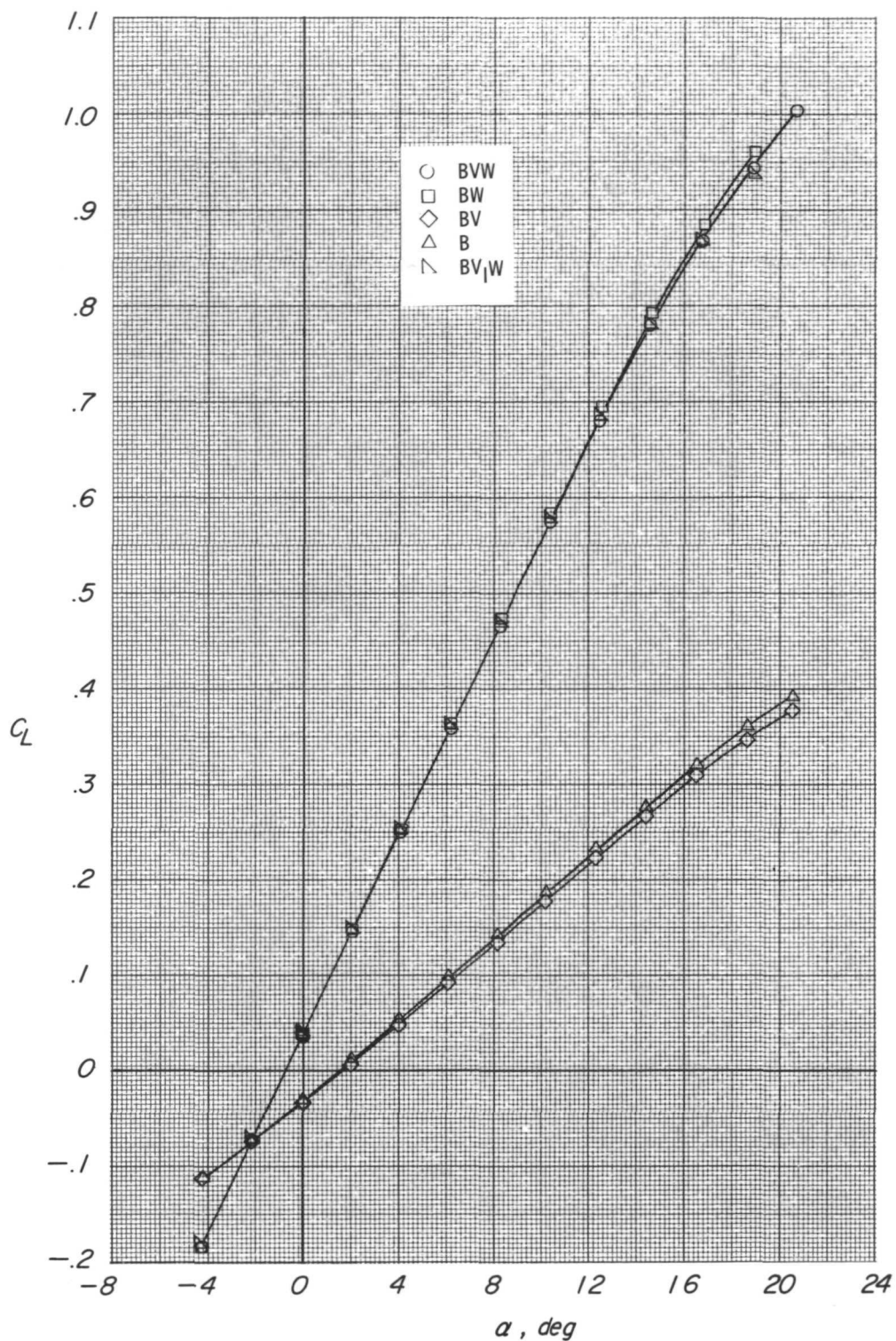
(a) Variation of lift coefficient with angle of attack.

Figure 4.- Longitudinal aerodynamic characteristics of complete model, wing-body combination, and body alone. $\Gamma = 0^O$; $\beta = 0^O$; $R = 22.13 \times 10^6$; $\delta_e = 0^O$; $\delta_f = 0^O$.
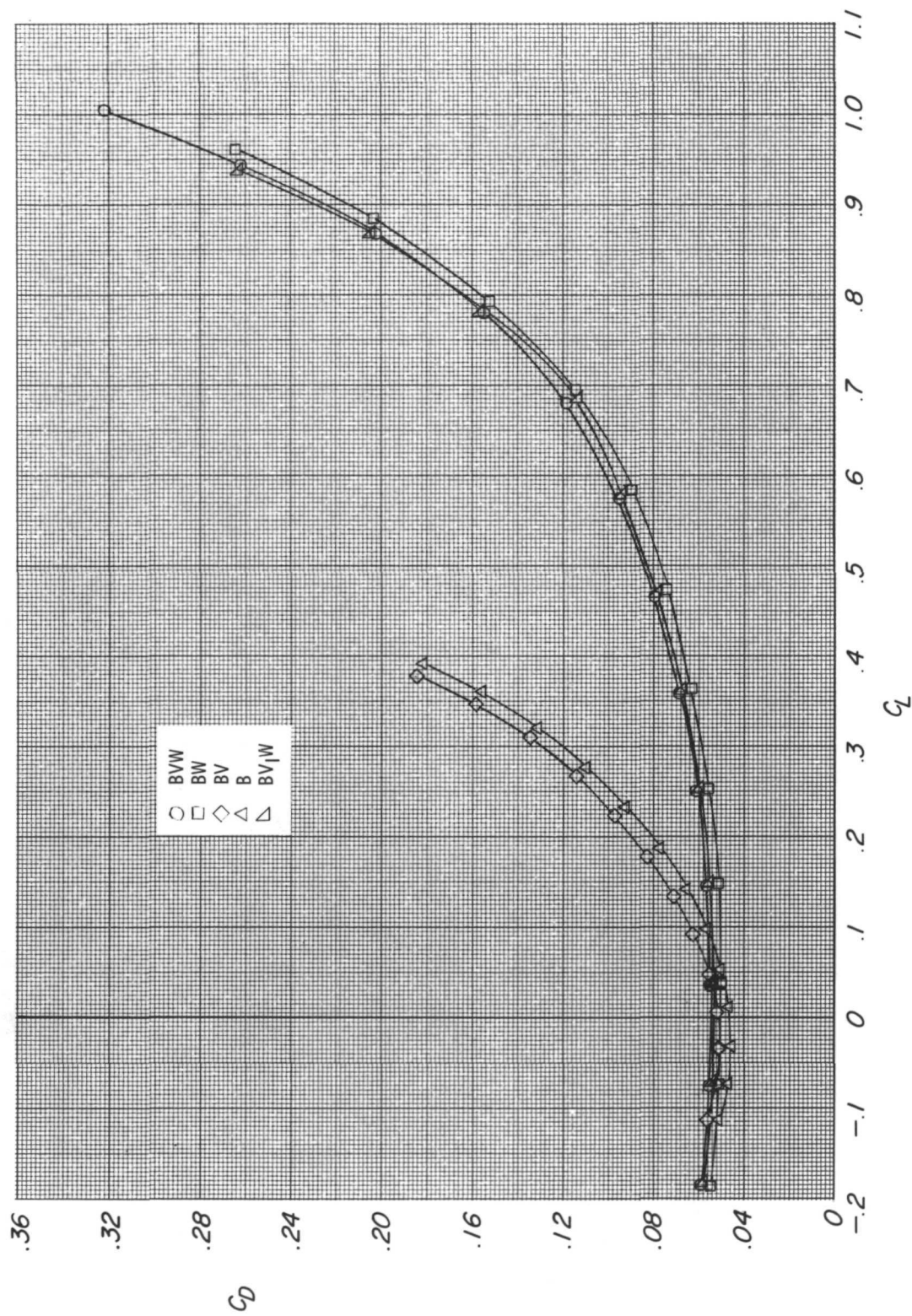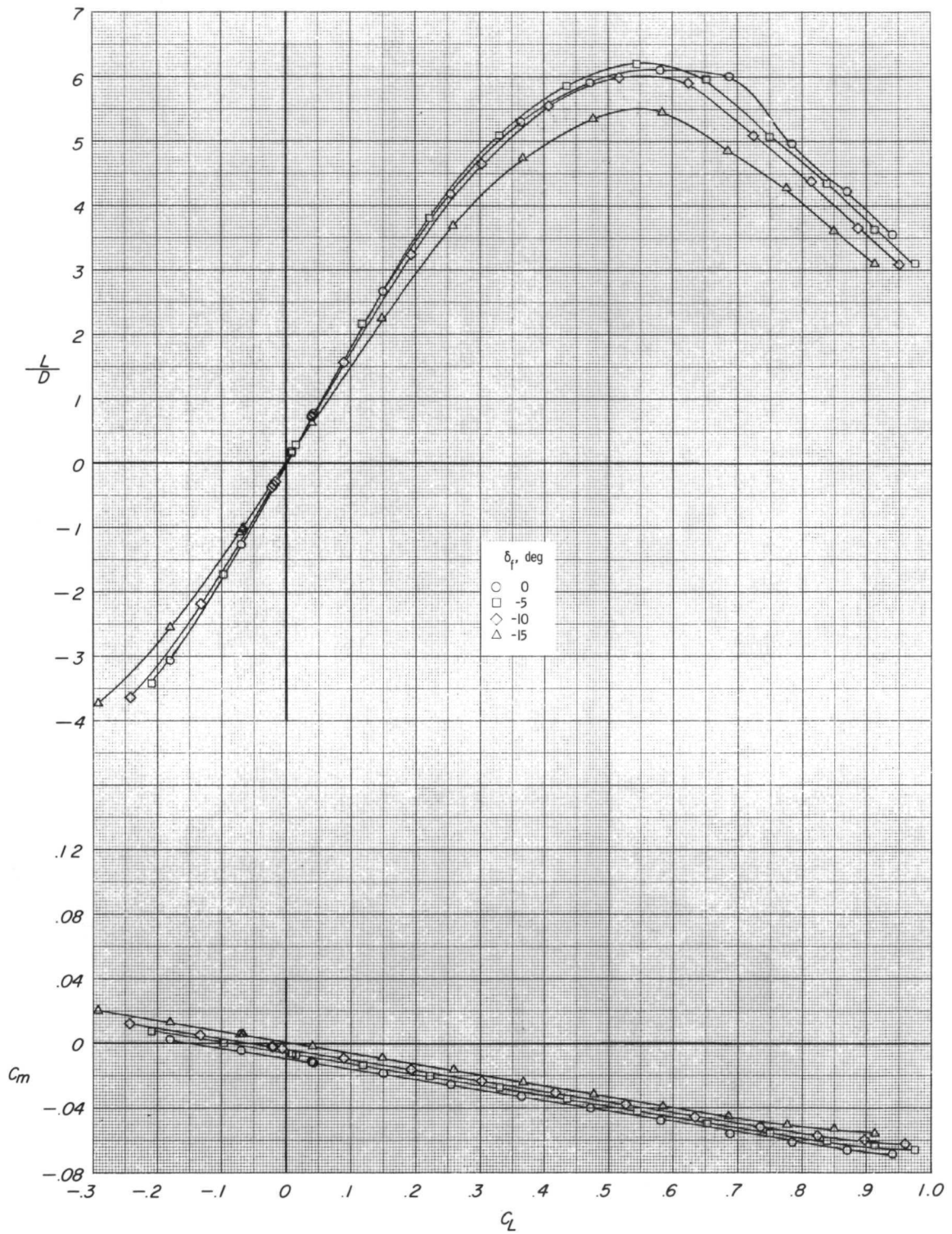
(b) Variation of drag coefficient with lift coefficient.
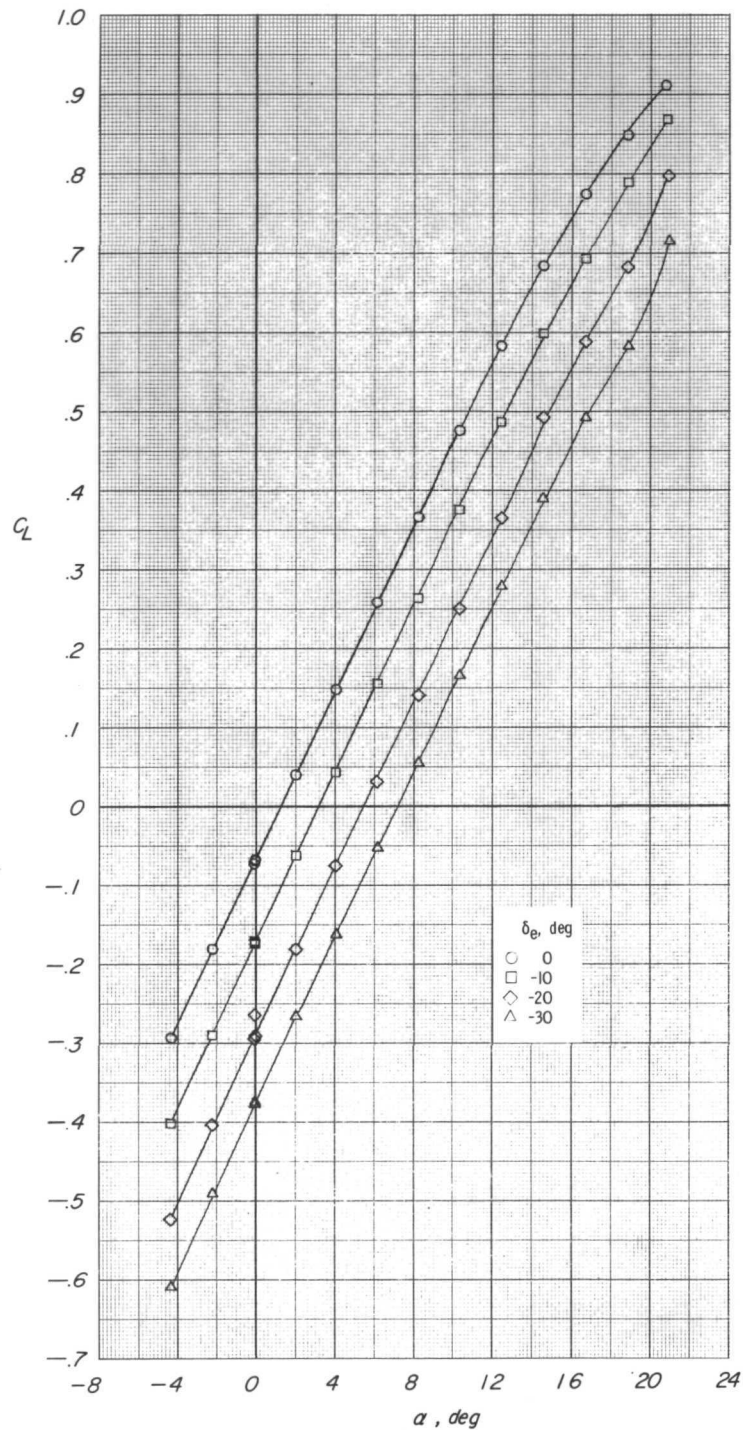
Figure 4.- Continued.
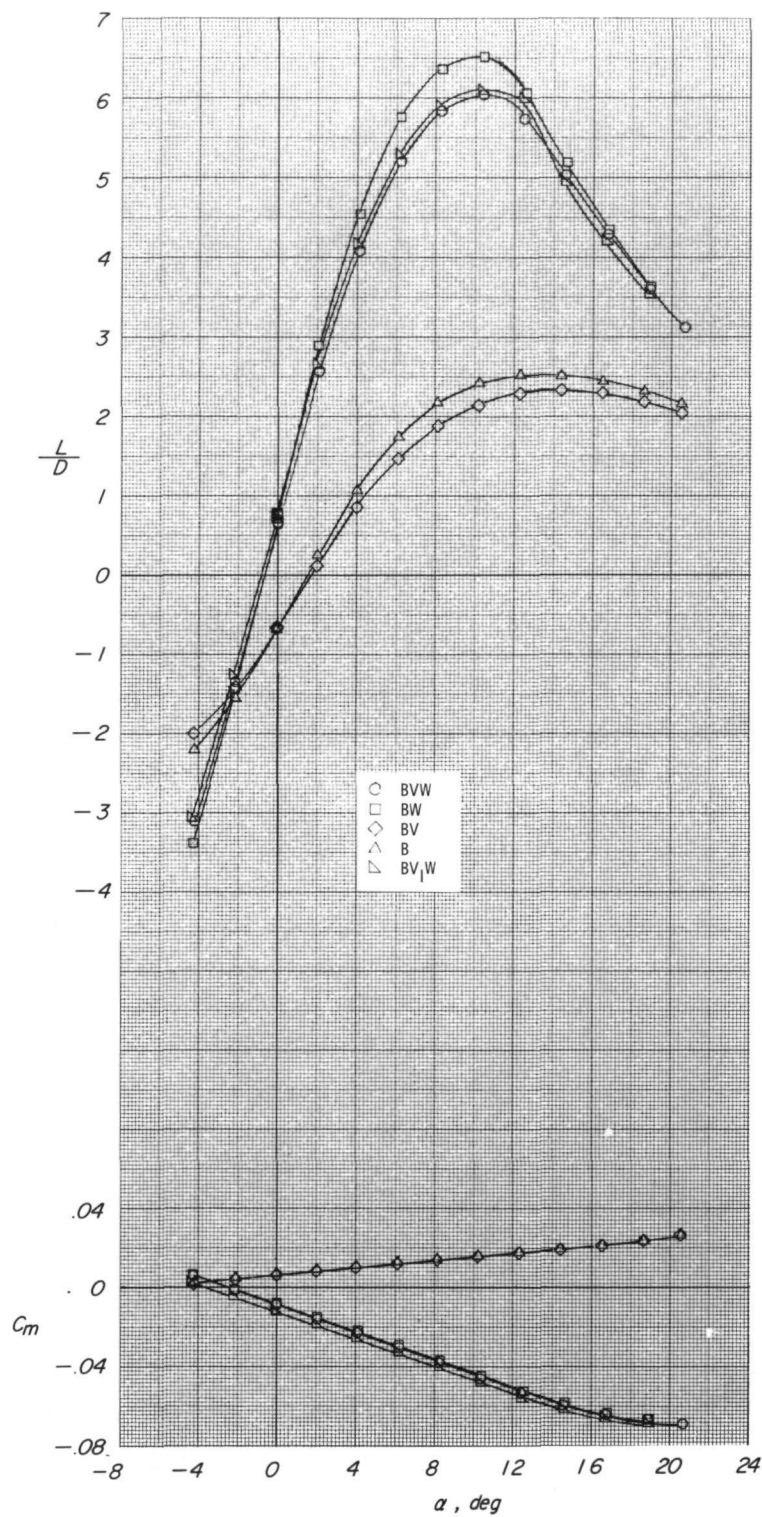
(c) Variation of lift-drag ratio and pitching-moment
coefficient with angle of attack.

Figure 4.- Continued.
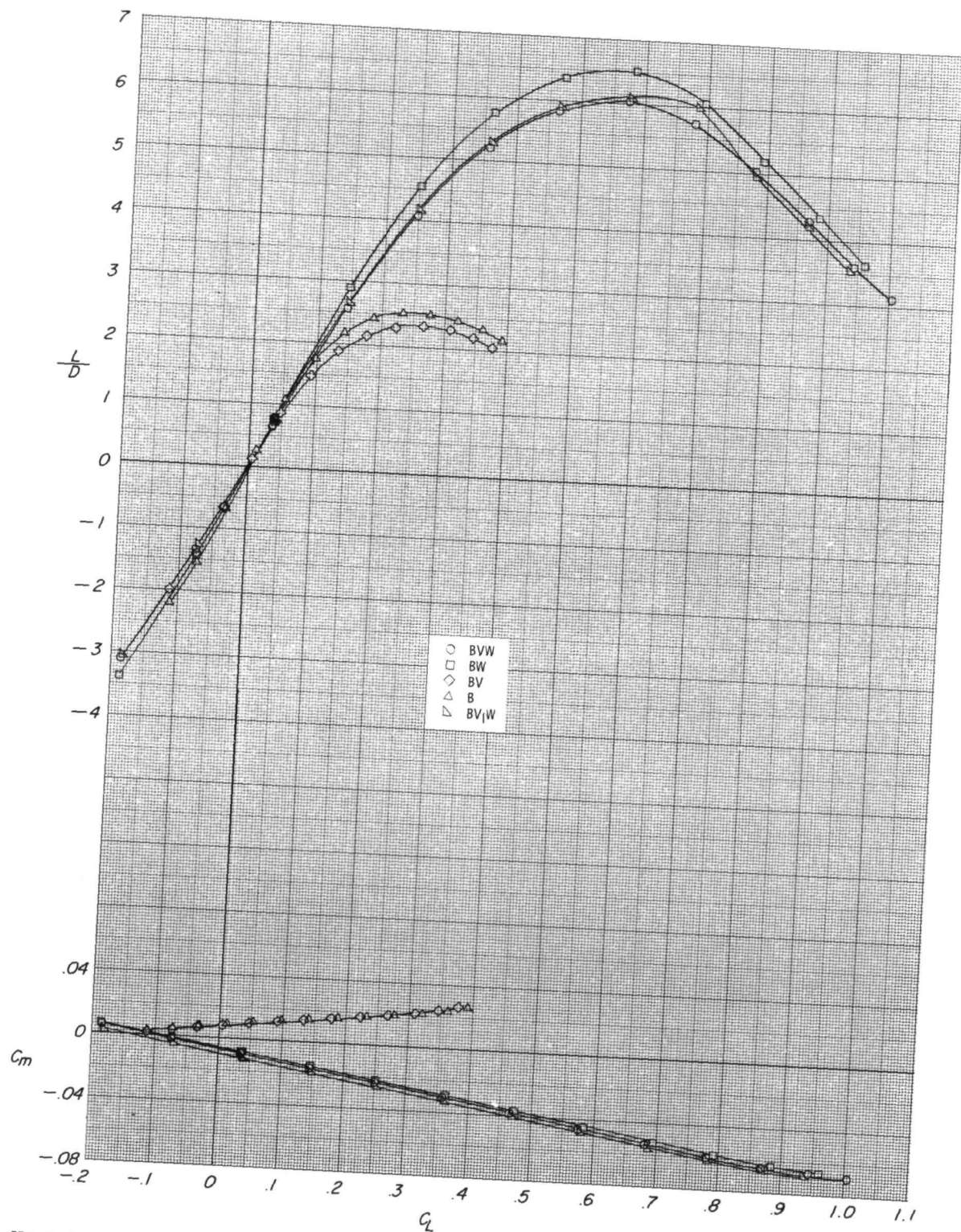
(d) Variation of lift-drag ratio and pitching-moment coefficient with lift coefficient.
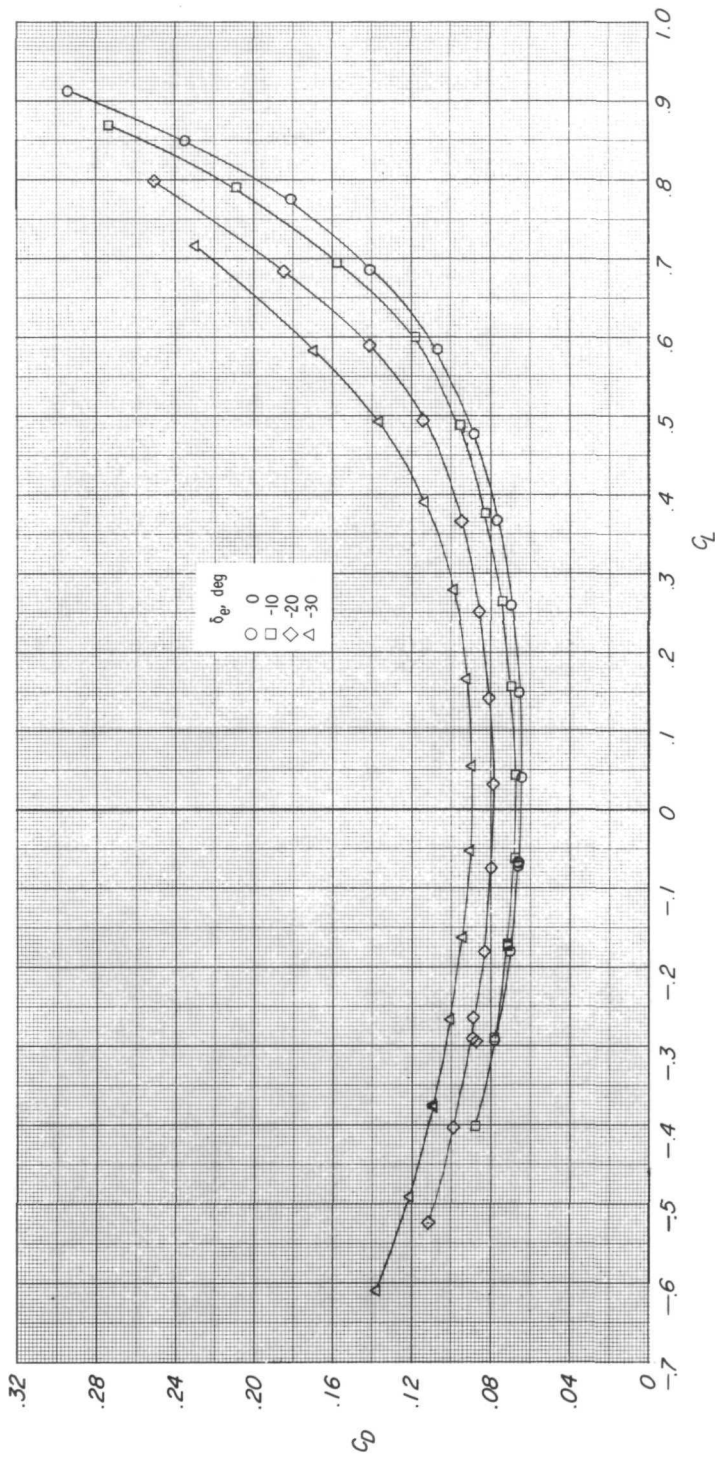
Figure 4.- Concluded.
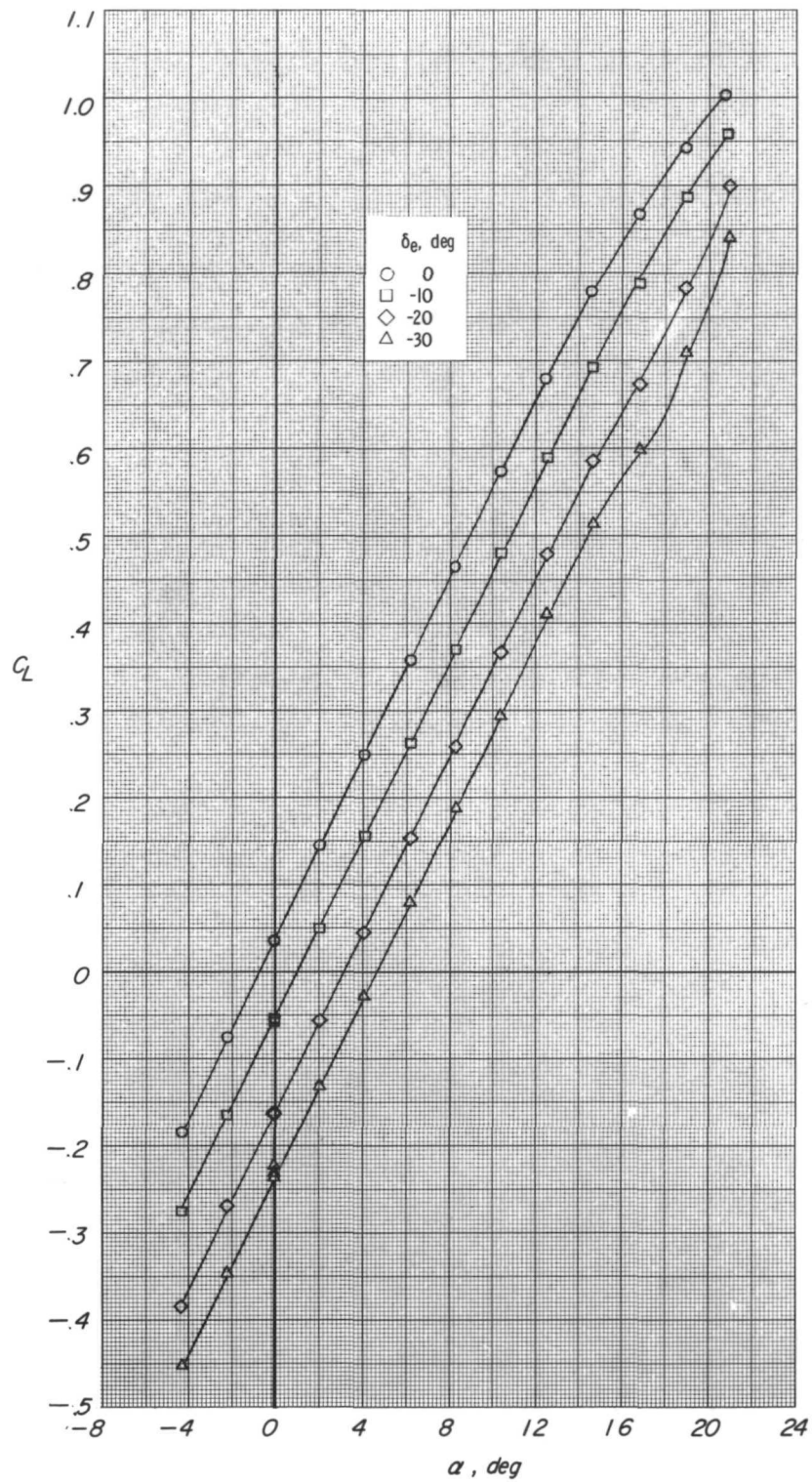
(a) Variation of lift coefficient with angle of attack.

Figure 5.- Effect of elevon deflection on longitudinal aerodynamic characteristics of model. Small vertical tail; $\Gamma = 0^\circ$; $\beta = 0^\circ$; $R = 22.13 \times 10^6$; $\delta_f = 0^\circ$.
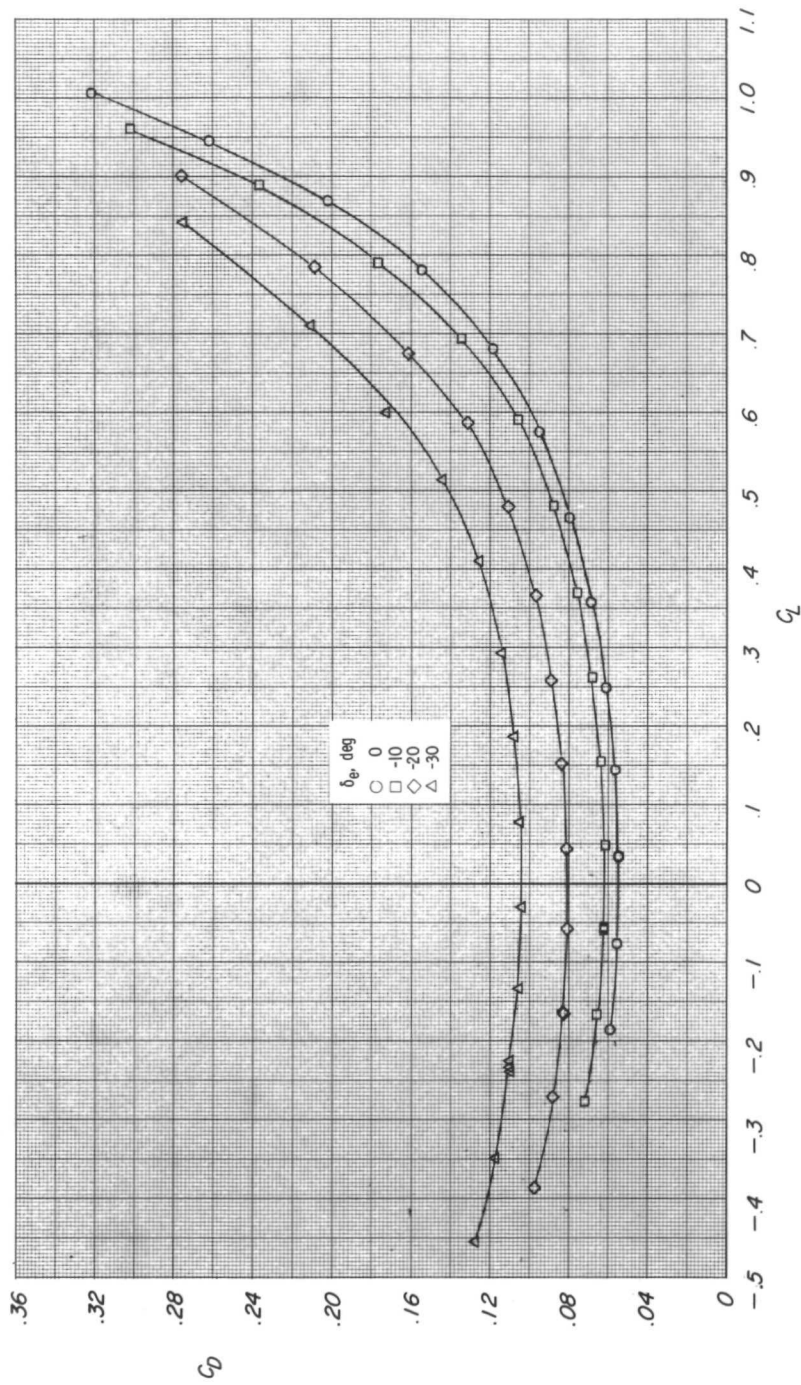
(b) Variation of drag coefficient with lift coefficient.

Figure 5.- Continued.
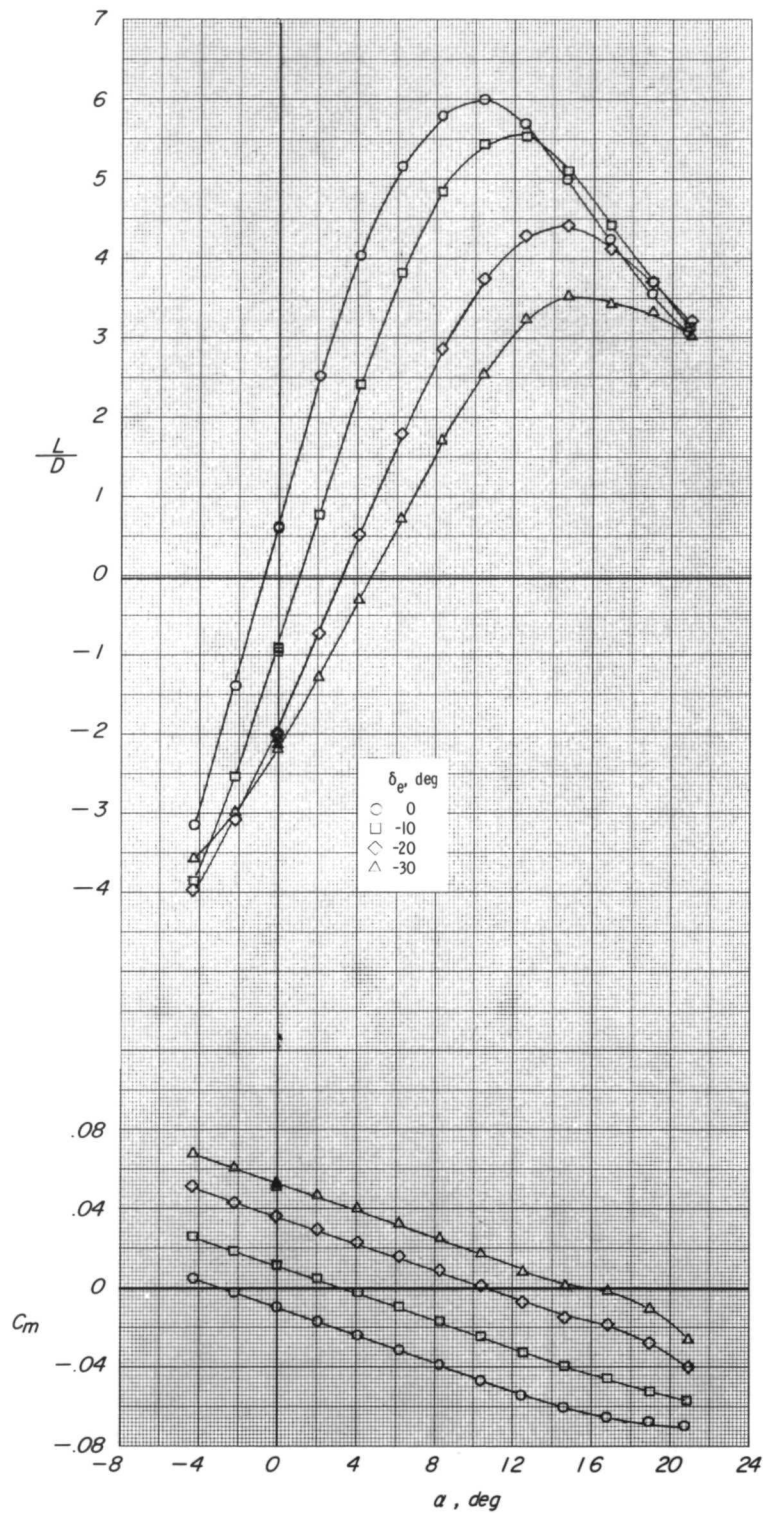
(c) Variation of lift-drag ratio and pitching-moment coefficient
with angle of attack.

Figure 5.- Continued.
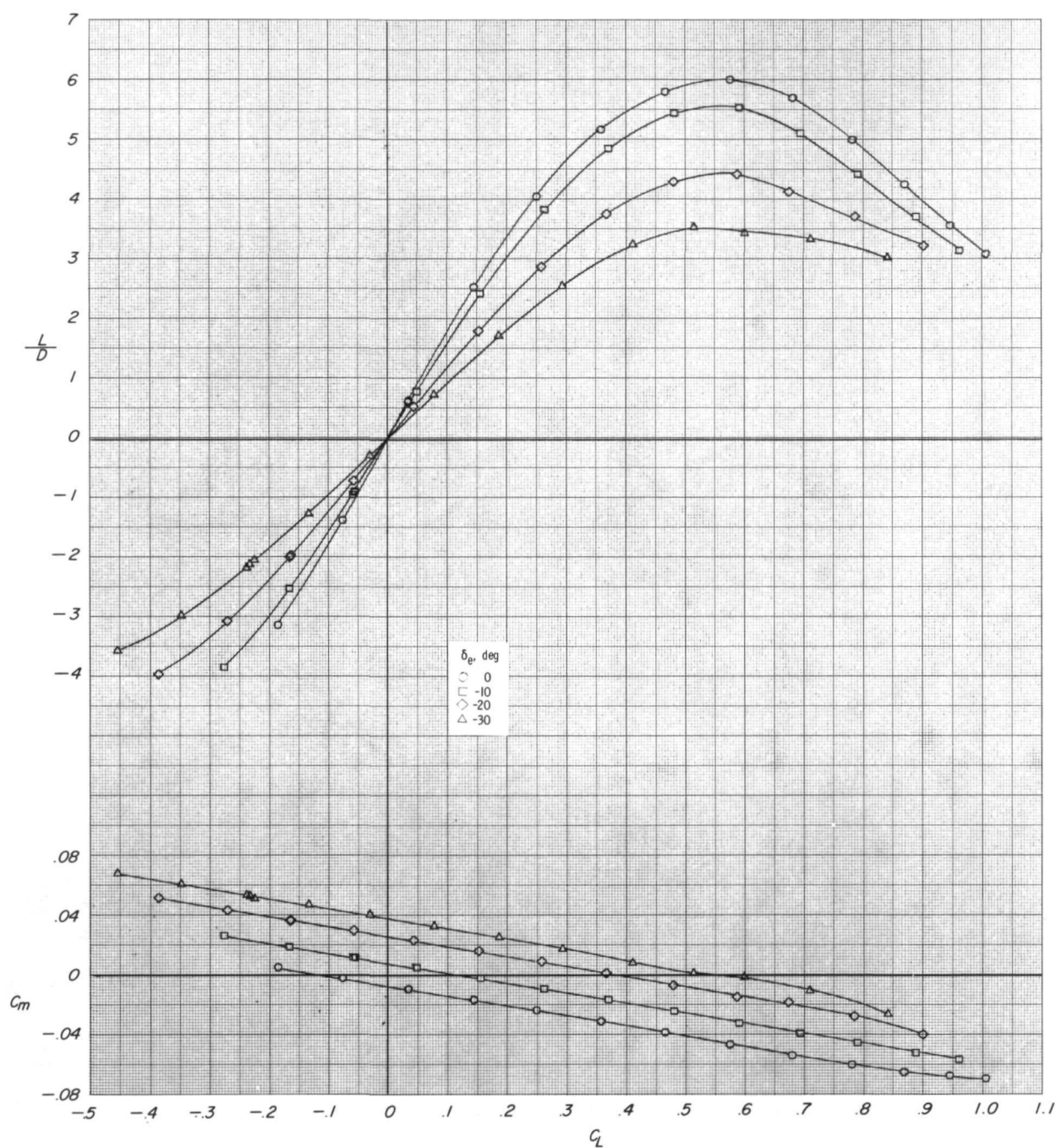
(d) Variation of lift-drag ratio and pitching-moment coefficient with lift coefficient.

Figure 5.- Concluded.
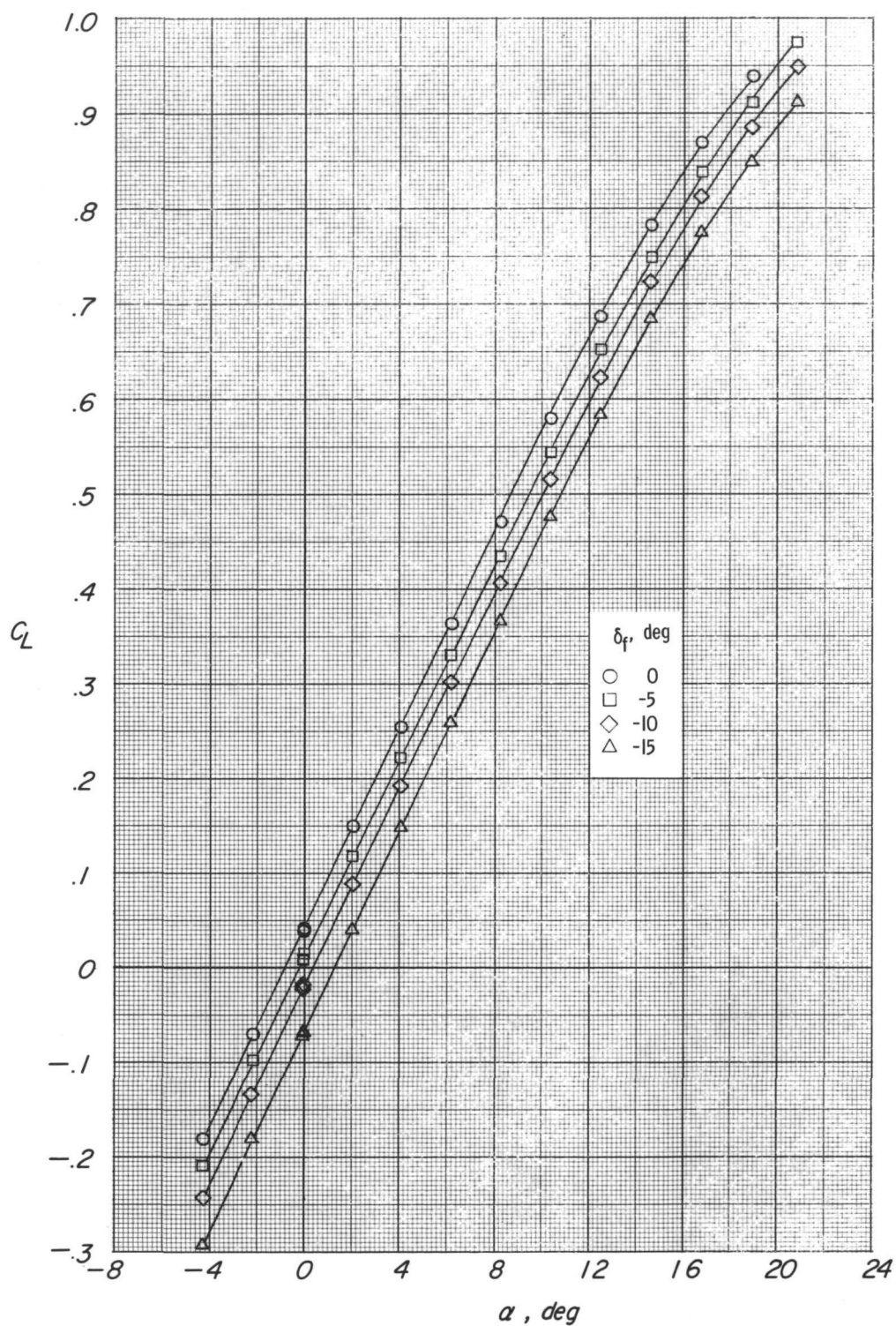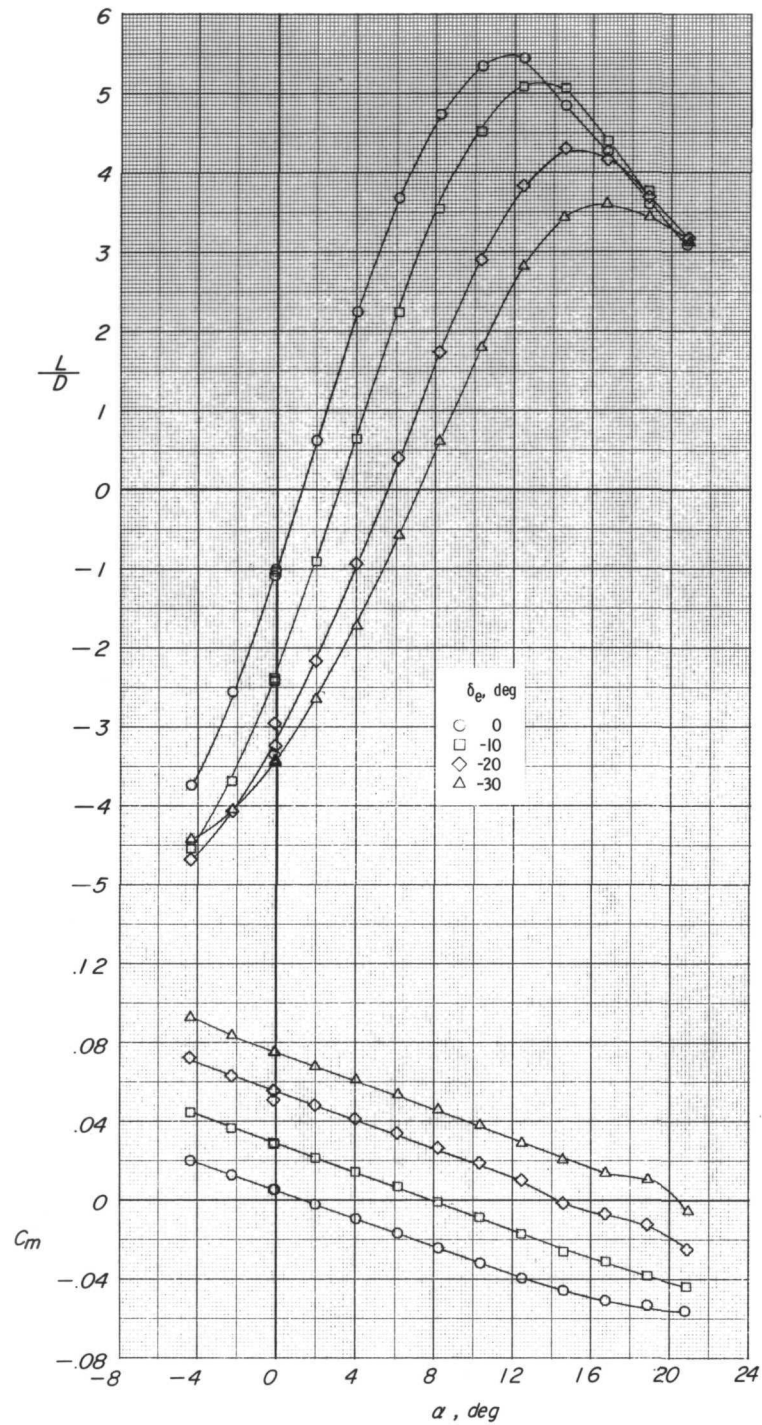
(a) Variation of lift coefficient with angle of attack.

Figure 6.- Effect of base-flap deflection on longitudinal aerodynamic
characteristics of model. Large vertical tail; $\Gamma = 0°$; $\beta = 0°$;
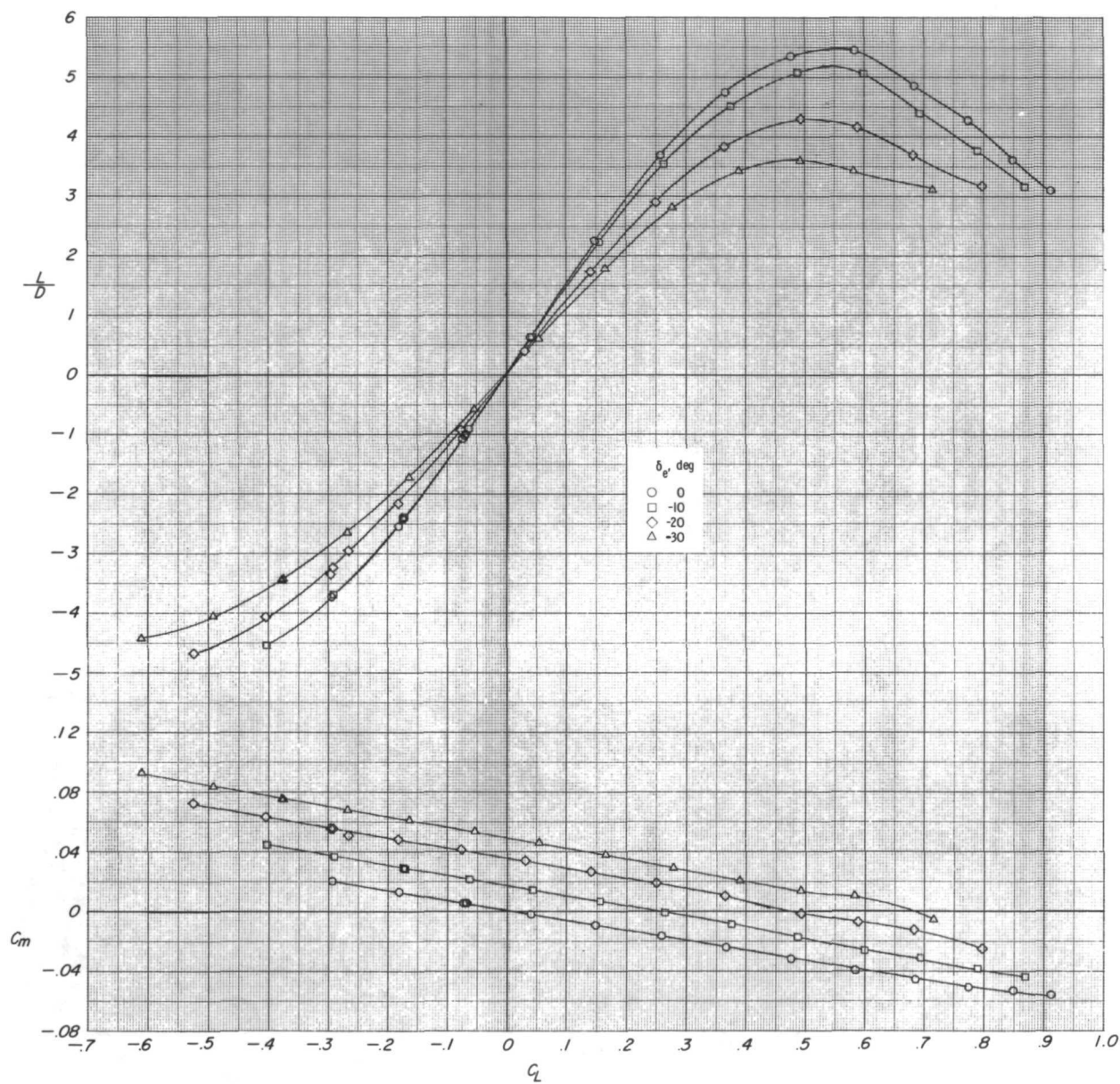$R = 22.13 \times 10^6$.

(b) Variation of drag coefficient with lift coefficient.

Figure 6.- Continued.

(c) Variation of lift-drag ratio and pitching-moment coefficient with angle of attack.

Figure 6.- Continued.

(d) Variation of lift-drag ratio and pitching-moment coefficient with lift coefficient.
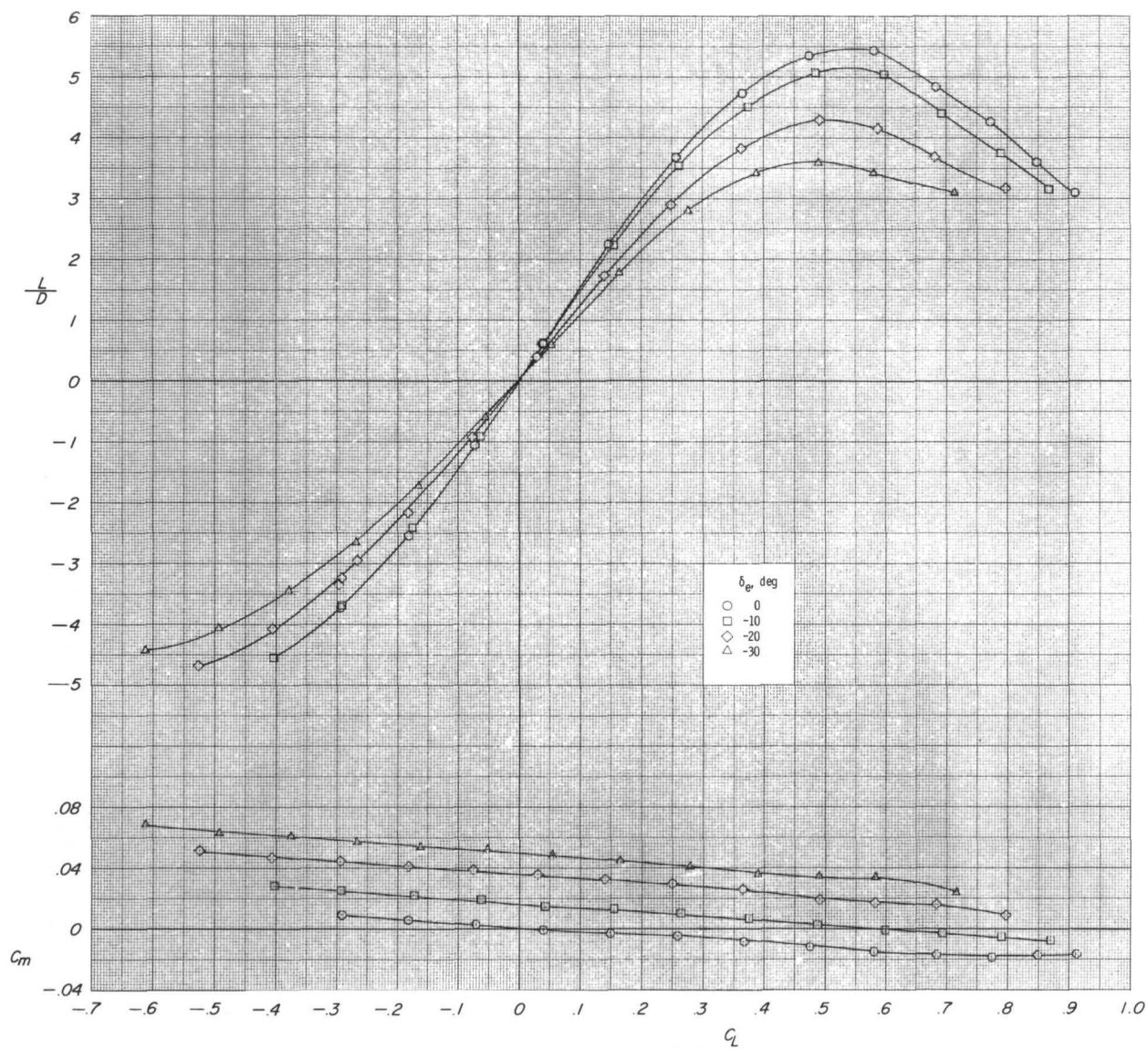
Figure 6.- Concluded.

(a) Variation of lift coefficient with angle of attack.

Figure 7.- Effect of elevon deflection in conjunction with base-flap
deflection on longitudinal aerodynamic characteristics of model.
Large vertical tail; $\Gamma = 0^\circ$; $\beta = 0^\circ$; $R = 22.13 \times 10^6$; $\delta_f = -15^\circ$.

(b) Variation of drag coefficient with lift coefficient.

Figure 7.- Continued.

(c) Variation of lift-drag ratio and pitching-moment coefficient
with angle of attack.

Figure 7.- Continued.

(d) Variation of lift-drag ratio and pitching-moment coefficient
with lift coefficient.

Figure 7.- Concluded.
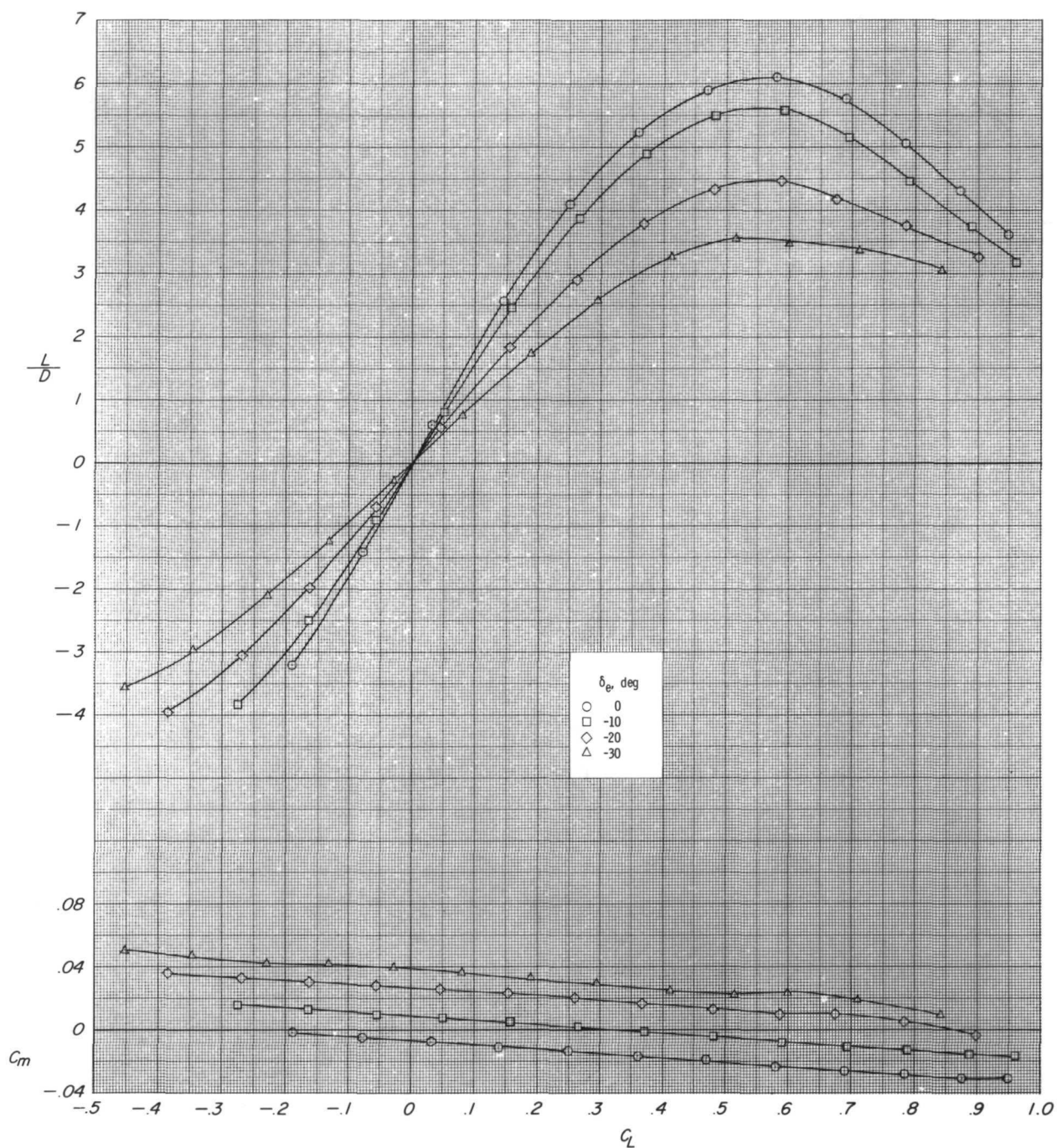
(a) Model with small vertical tail; $\delta_f = 0°$.

Figure 8.- Longitudinal aerodynamic characteristics of model with center of gravity at $0.74l$. $\beta = 0°$; $R = 22.13 \times 10^6$.

(b) Model with large vertical tail; $\delta_f = -15°$.

Figure 8.- Concluded.
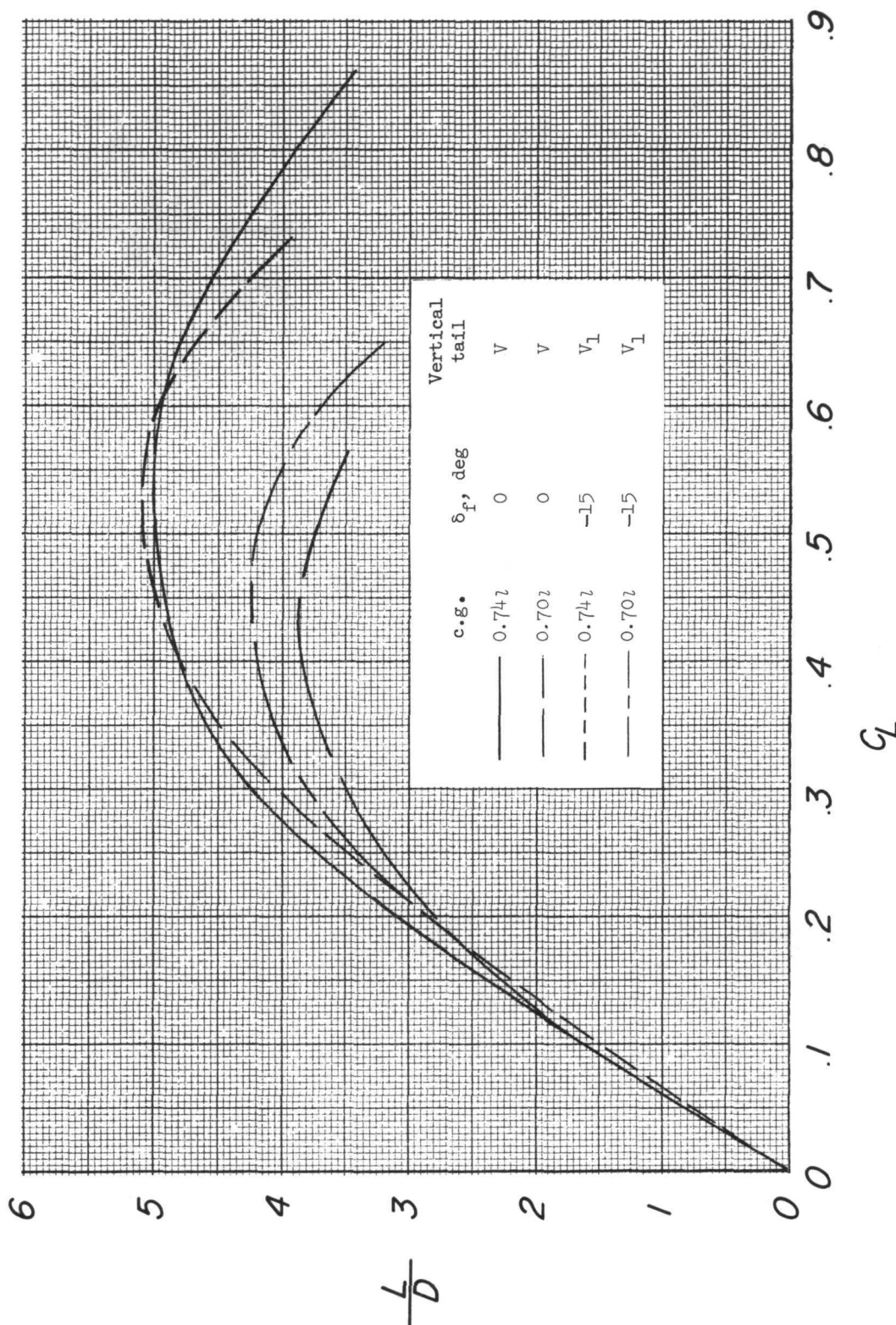
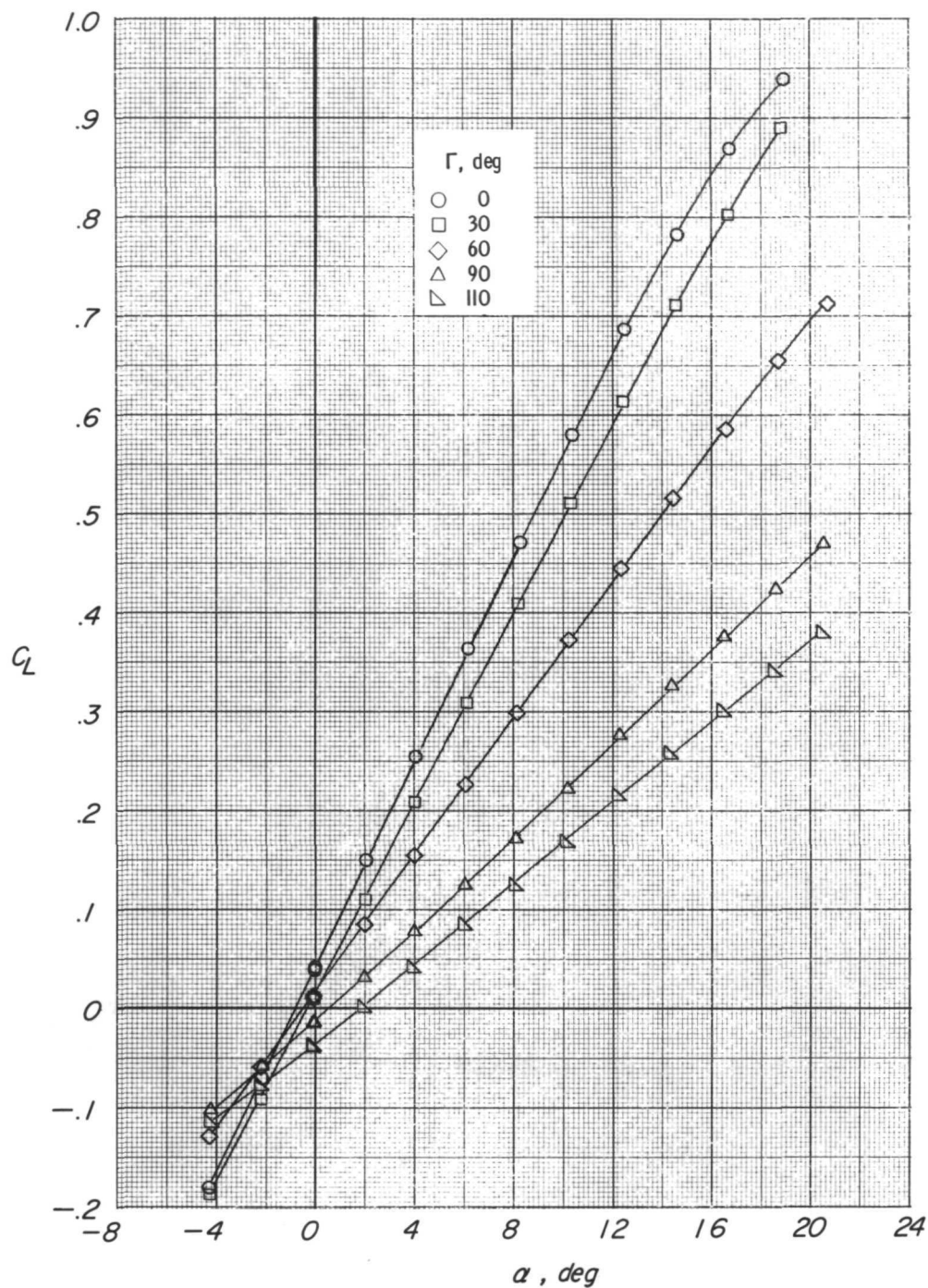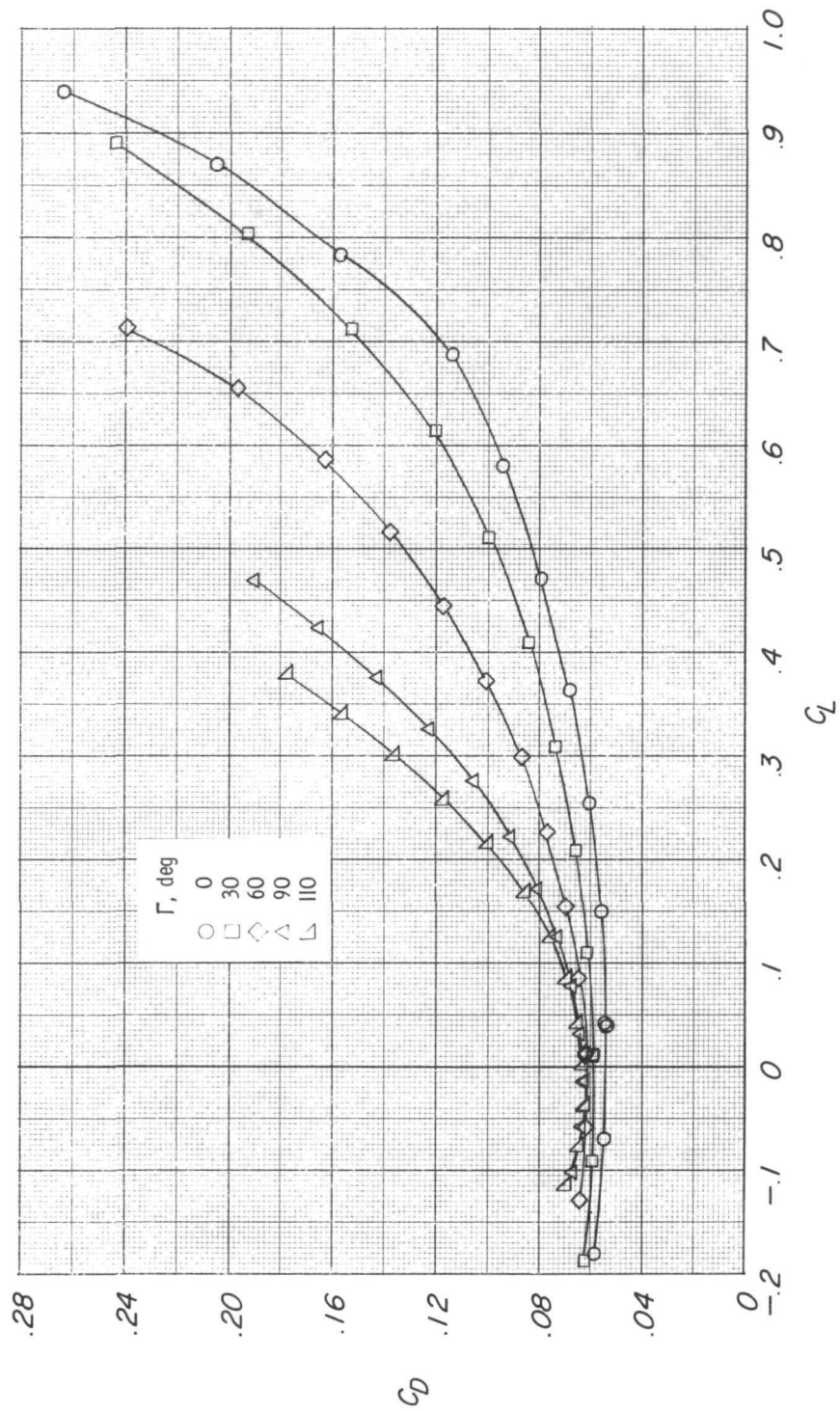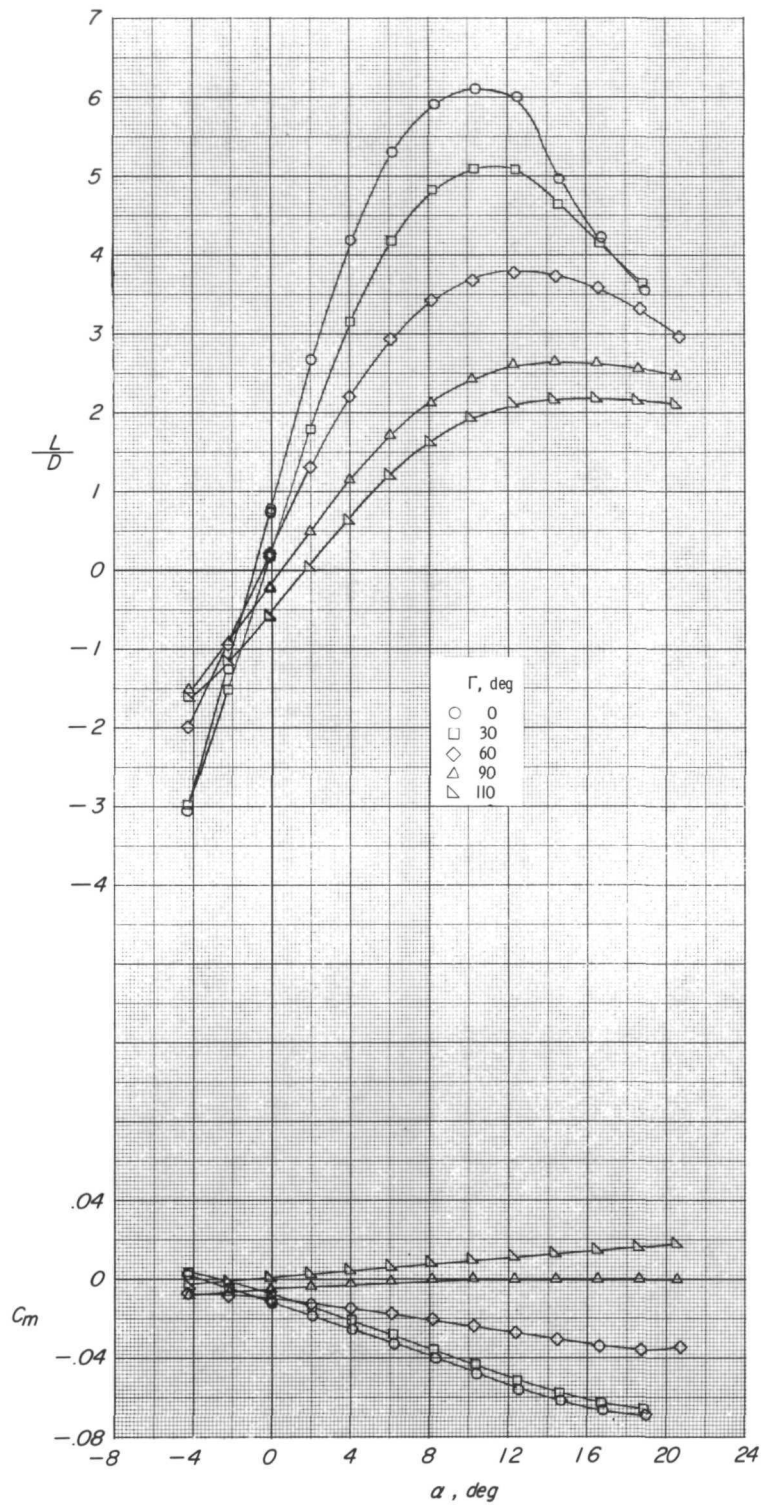Figure 9.- Summary of longitudinal trim characteristics of model.

(a) Variation of lift coefficient with angle of attack.

Figure 10.- Effect of wing dihedral angle on longitudinal aerodynamic characteristics of model. Large vertical tail; $\beta = 0^{\text{o}}$; $R = 22.13 \times 10^6$; $\delta_f = 0^{\text{o}}$.
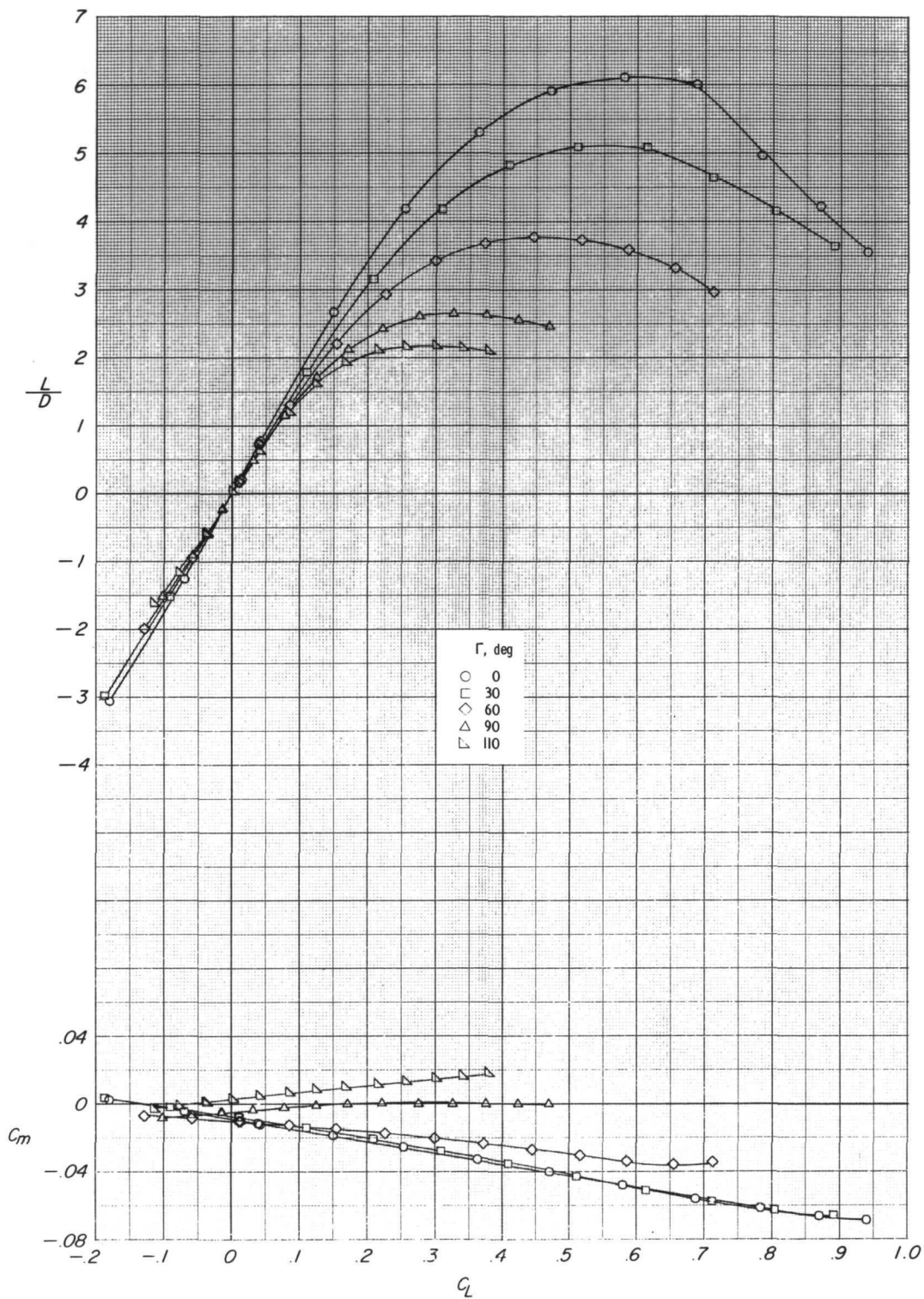
(b) Variation of drag coefficient with lift coefficient.

Figure 10.- Continued.

(c) Variation of lift-drag ratio and pitching-moment coefficient
with angle of attack.

Figure 10.- Continued.

(d) Variation of lift-drag ratio and pitching-moment coefficient
with lift coefficient.
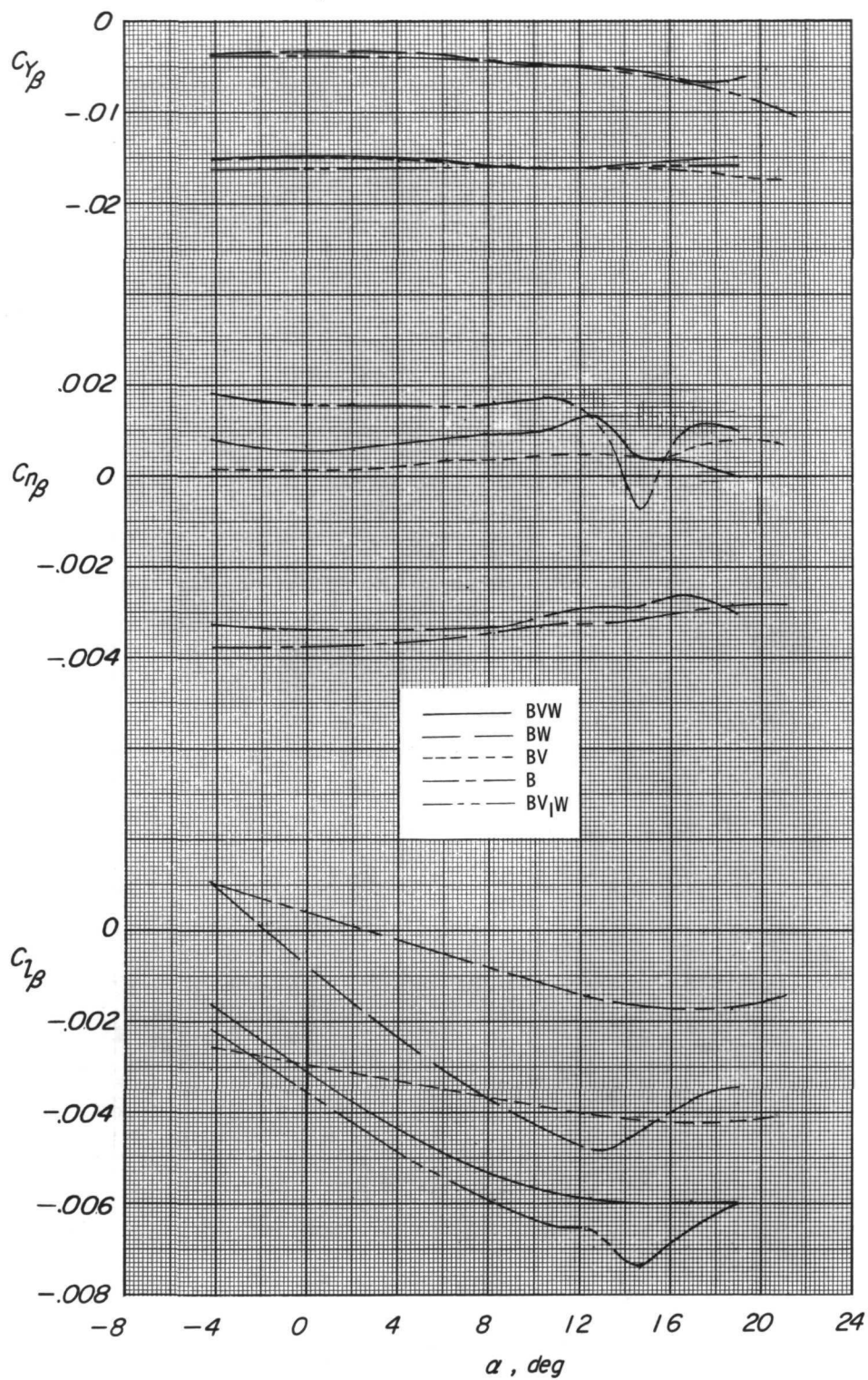
Figure 10.- Concluded.

Figure 11.- Lateral-directional stability characteristics of complete model, wing-body combination, and body alone. $\Gamma = 0^o$; $\beta = 0^o$; $R = 22.13 \times 10^6$.
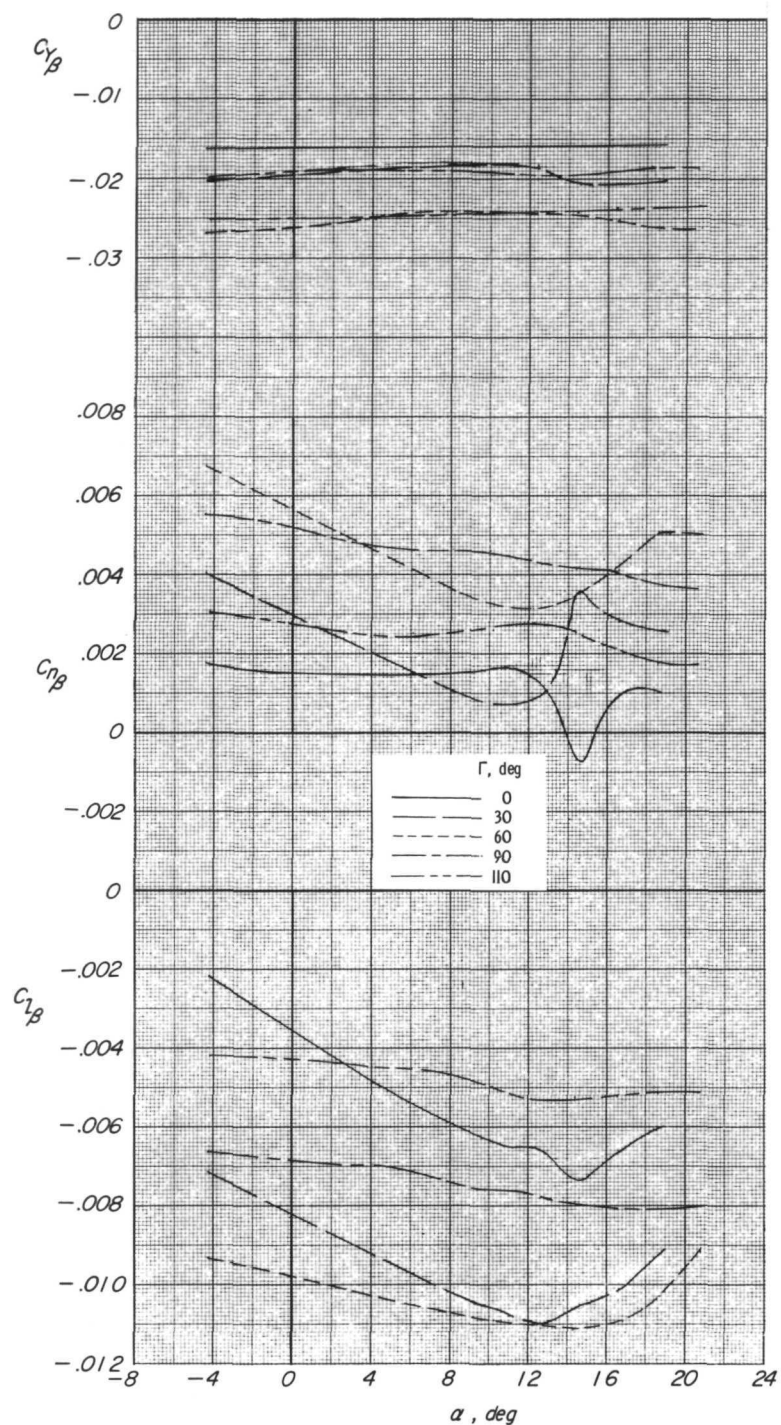
Figure 12.- Effect of wing dihedral angle on lateral-directional
stability characteristics of model. Large vertical tail;
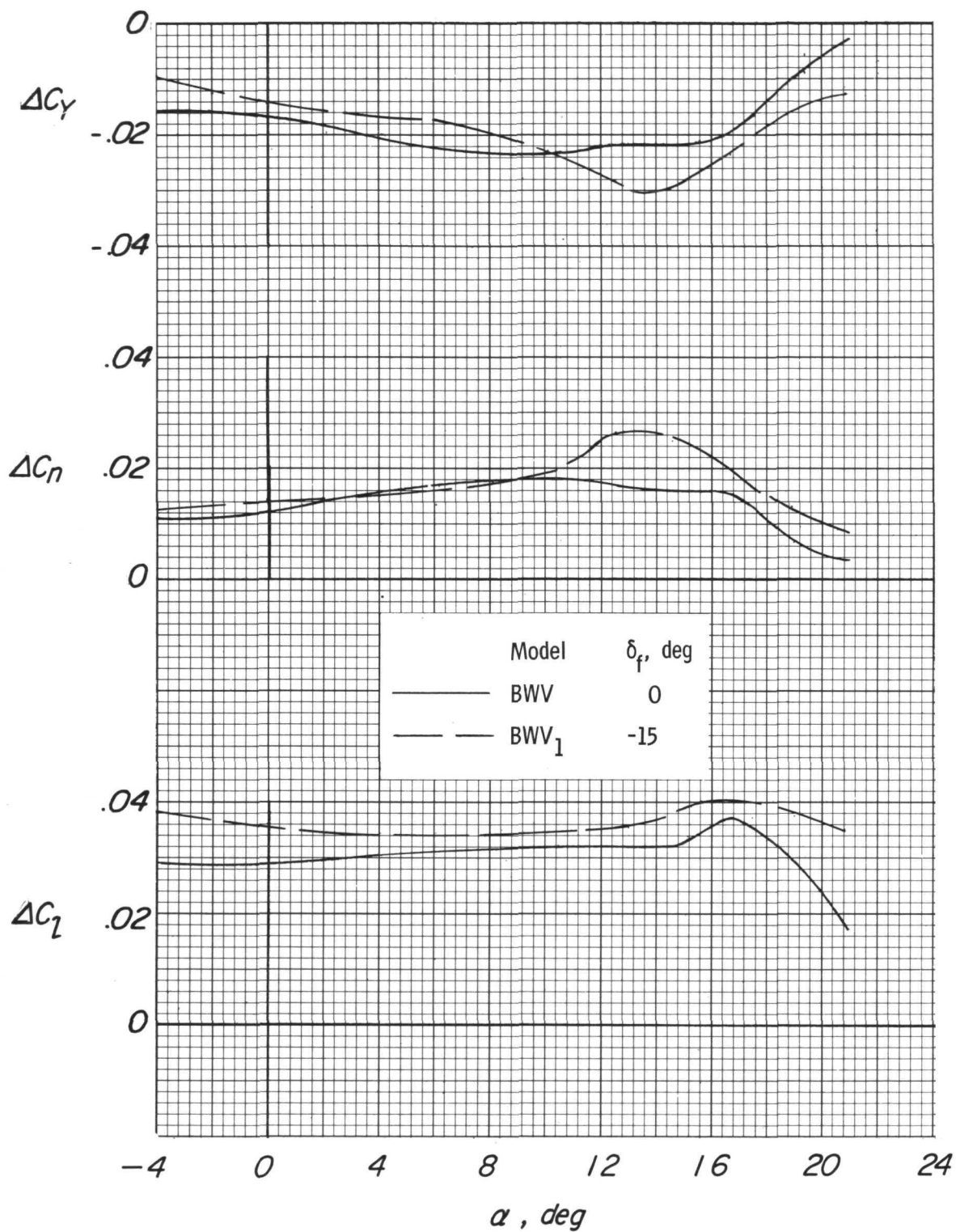$R = 22.13 \times 10^6$; $\delta_f = 0^\circ$.

Figure 13.- Effect of differential elevon deflection as a roll control on lateral aerodynamic characteristics of model. $\delta_{e,R} = -10°$; $\delta_{e,L} = -30°$; $\Gamma = 0°$; $\beta = 0°$; $R = 22.13 \times 10^6$.

Page Intentionally Left Blank

*"The aeronautical and space activities of the United States shall be
conducted so as to contribute . . . to the expansion of human knowl-
edge of phenomena in the atmosphere and space. The Administration
shall provide for the widest practicable and appropriate dissemination
of information concerning its activities and the results thereof."*

—NATIONAL AERONAUTICS AND SPACE ACT OF 1958

NASA SCIENTIFIC AND TECHNICAL PUBLICATIONS

TECHNICAL REPORTS: Scientific and
technical information considered important,
complete, and a lasting contribution to existing
knowledge.

TECHNICAL NOTES: Information less broad
in scope but nevertheless of importance as a
contribution to existing knowledge.

TECHNICAL MEMORANDUMS:
Information receiving limited distribution
because of preliminary data, security classifica-
tion, or other reasons.

CONTRACTOR REPORTS: Scientific and
technical information generated under a NASA
contract or grant and considered an important
contribution to existing knowledge.

TECHNICAL TRANSLATIONS: Information
published in a foreign language considered
to merit NASA distribution in English.

SPECIAL PUBLICATIONS: Information
derived from or of value to NASA activities.
Publications include conference proceedings,
monographs, data compilations, handbooks,
sourcebooks, and special bibliographies.

**TECHNOLOGY UTILIZATION
PUBLICATIONS:** Information on technology
used by NASA that may be of particular
interest in commercial and other non-aerospace
applications. Publications include Tech Briefs,
Technology Utilization Reports and
Technology Surveys.

Details on the availability of these publications may be obtained from:

SCIENTIFIC AND TECHNICAL INFORMATION OFFICE

NATIONAL AERONAUTICS AND SPACE ADMINISTRATION
Washington, D.C. 20546